

# Palynology and palynofacies studies in the lowermost Jurassic of the Lusitanian Basin (Pereiros Formation of the Silves Group), Portugal: evidence of the first transgressive episode

MARGARIDA VILAS-BOAS<sup>1\*</sup>, ZÉLIA PEREIRA<sup>2</sup>, SIMONETTA CIRILLI<sup>3</sup>,  
LUÍS VÍTOR DUARTE<sup>4</sup>, SÉRGIO LUIS RODRIGUES SÊCO<sup>5</sup> and PAULO FERNANDES<sup>1</sup>

<sup>1</sup>CIMA, Centre of Marine and Environmental Research/ARNET – Infrastructure Network in Aquatic Research, University of Algarve, Campus de Gambelas, 8000-139 Faro, Portugal; e-mails: amvilasboas@ualg.pt, ORCID: 0000-0001-8501-7052; pfernandes@ualg.pt

<sup>2</sup>LNEG, Rua da Amieira, 4465-965 S. Mamede de Infesta, Porto, Portugal; e-mail: zelia.pereira@lneg.pt

<sup>3</sup>Department of Physics and Geology, Università degli Studi di Perugia, 06123 Perugia, Italy; e-mail: simonetta.cirilli@unipg.it

<sup>4</sup>University of Coimbra, MARE – Marine and Environmental Sciences Centre/ARNET – Infrastructure Network in Aquatic Research, Rua Sílvio Lima, 3030-790 Coimbra, Portugal; e-mail: lduarte@det.ucp

<sup>5</sup>University of Coimbra, IDL – Instituto Dom Luiz, LRN-Laboratory of Natural Radioactivity, Department of Earth Sciences, Coimbra, Portugal; e-mail: osergioseco@gmail.com

Received 25 May 2023; accepted for publication 17 October 2023

**ABSTRACT.** The Silves Group of the Lusitanian Basin in Portugal represents the initial infill of the continental rifting basins that formed during the breakup of northern Pangaea regions. Evaporites, especially halite, mark the transition from continental to marine settings and the beginning of the deposition in passive margin basins. This work presents the results of the palynostratigraphic and palynofacies analysis of two partial sections from the Pereiros Formation at the top of the Silves Group. The two sections are composed of sandstones, mudstones and dolostones interpreted as deposited in fluvial and lacustrine settings without apparent marine influence. The palynological content is diverse and wellpreserved, dating both sections to the early Hettangian (Lower Jurassic), indicated by the presence of spores *Ischyosporites variegatus*, *Kraeuselisporites reissingeri*, *Porcellispora longdonensis* and the pollen grains *Perinopollenites elatoides* and *Pinuspollenites minimus*. The palynological content of one of the sections (Lamas I) is noticeable by microforaminifera linings, suggesting evidence for a hitherto marine incursion at this age in the Silves Group stratigraphy. The beds that yielded the microforaminifera linings are interpreted as having been deposited in an estuarine-type setting, created by the first and short-lived marine transgressive event in the Lusitanian Basin during the early Hettangian.

**KEYWORDS:** Microforaminifera linings, Rift Basin, Marine Transgression, Estuary, Hettangian, Tethys Realm

## INTRODUCTION

Pangea's breakup caused the early stages of the North Atlantic opening. In the western Iberian sector, the Lusitanian Basin (LB) begins to develop, flanked to the east by reliefs left over from the late phases of the Variscan

orogeny (see, for example, Wilson, 1975, 1988; Hiscott et al., 1990; Kullberg et al., 2013).

The basin infill of the Mesozoic in Portugal has been identified as the base unit of the Silves Group that is primarily siliciclastic, composed of coarse-grained pebbly arkoses to feldspar litharenites (Palain, 1976; Soares et al.,

\* Corresponding author

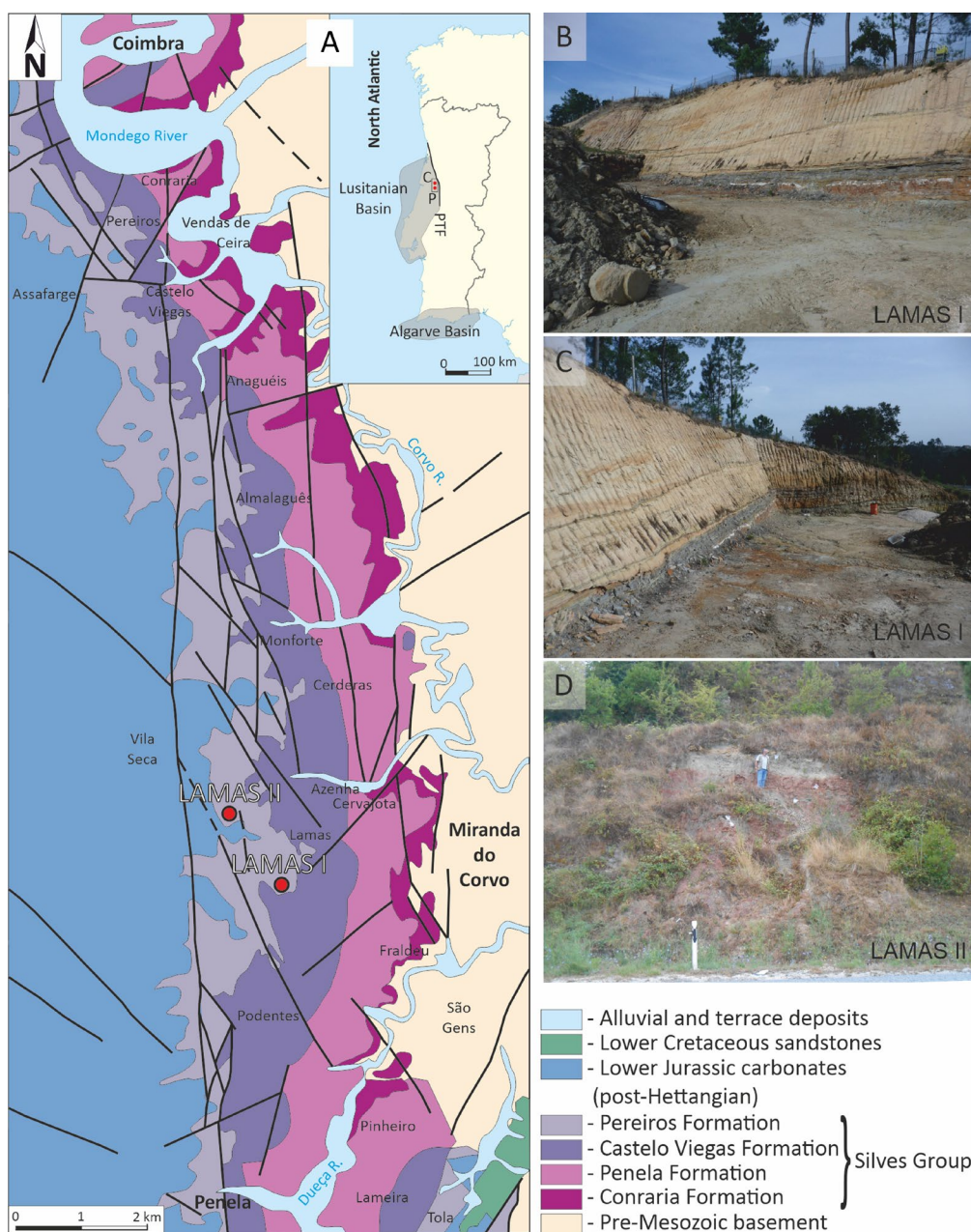


**Figure 1.** A. Map of Portugal with the rectangle highlighting the type-area of the Silves Group in the Lusitanian Basin (PTF – Porto-Tomar Fault, C – Coimbra, P – Penela) and map of the study area with the location of the studied sections (LAMAS I and LAMAS II) (based on Soares et al., 2012); B, C. Photographs from the Lamas I section; D. Photograph from the Lamas II section

2007, 2012). The main continuous outcrop area of this Group in the LB is approximately 3 to 4 km wide and 35 km long from Coimbra to Penela (Fig. 1). The Silves Group comprehends four formations, from the oldest to the most recent: the Conraria, Penela, Castelo Viegas and Pereiros formations (Soares et al., 2012) (Fig. 2). Only a few palynostratigraphic studies have been performed in the Silves Group of the LB. Döbinger et al. (1970) carried out the initial investigation that was later continued by Adloff et al. (1974), who used Palain's sedimentology and allostratigraphy work applying the traditional definition in megasequences A,

B and C (Palain, 1976, 1979). Recent palynological data from these formations allowed better age detailing, dating the Conraria Formation as Norian (late Triassic) and the Pereiros Formation as Hettangian (early Jurassic; Vilas-Boas et al., 2021). The first marine record (*Isocyprina* Beds; B2 term in Palain) caused a significant alteration in the sedimentary record of the Pereiros Formation, with the uppermost part referring to transitional intertidal settings (Soares et al., 2012).

The Triassic–Jurassic Boundary (TJB) ( $201.4 \pm 0.2$  My; Gradstein and Ogg, 2020) corresponds to one of the most severe biotic crises

Palain (1976)	Soares et al. (2012)	Vilas-Boas et al. (2021)	This work
Coimbra Formation			
C2	Pereiros Formation	Hettangian	Lamas II
C1 (10 m)			
B2 (6 m)			
		?	TJB
		Rhaetian	
		?	
B1 (210 m)	Castelo Viegas Formation		D
	Penela Formation		
A2 (80 m)	Conraria Formation	Norian	
A1 (100–140 m)			?

**Figure 2.** Chronostratigraphic table of the Silves Group. D – Discontinuity; TJB – Triassic–Jurassic Boundary

of the Phanerozoic (Raup and Sepkoski, 1982; Sepkoski, 1996; Tanner et al., 2004), supported by high-resolution studies that demonstrate a significant change in the palynoflora during this time (Lindström, 2016; Lindström et al., 2017a, b, 2021). However, some recent palynological and macrofloristic studies also demonstrate that Europe has no indications of a significant extinction occurring across the TJB (Barbacka et al., 2017). An important marker of the end of Triassic in some places like Portugal, North Africa and Eastern North America is the magmatic activity of the Large Igneous Province of the Central Atlantic Magmatic Province (CAMP). The CAMP in Portugal is evidenced by the Messejana Dike (Wilson and Giraud, 1998) and a Volcano-Sedimentary Complex in the Algarve Basin (Verati et al., 2007; Martins et al., 2008). There is no direct evidence of the CAMP in the LB, except for the southernmost part of the basin (Azerêdo et al., 2003; Kullberg et al., 2013). Nevertheless, the secondary effects of the volcanism, such as acid rain, the acidification of freshwater and global warming due to greenhouse effect, are factors that contributed to the climatic changes and may have had an impact on the flora of this age (Hesselbo et al., 2002; Guex et al., 2004; Marzoli et al., 2004;

Tanner et al., 2004, 2007; Nomade et al., 2007; Schaltegger et al., 2008; Van de Schootbrugge et al., 2008, 2009; Cirilli et al., 2009, 2015, 2018; Deenen et al., 2010; Lindström, 2016; Davies et al., 2017; Lindström et al., 2019; Panfili et al., 2019; Capriolo et al., 2020). Furthermore, the increase in tectonic activity and changes in sea level at the TJB are also related to numerous sedimentary hiatuses in the Western European basins (Lindström et al., 2017a, b; Schneebeil-Hermann et al., 2018).

In the present research, palynostratigraphic and palynofacies analyses were made from two sections from the Silves Group of the LB in the Coimbra region (Fig. 1). This study aims to document the base of the Hettangian in the Lusitanian Basin, comment on its biostratigraphical and palaeoenvironmental significance based on palynostratigraphy and palynofacies analyses, with emphasis on sea-level changes as documented by the palynological and sedimentary records. This data complements palynological research conducted previously in the same region (specifically the LAM section in Vilas-Boas et al., 2021).

## GEOLOGICAL SETTING

The Triassic and Lower Jurassic sedimentary units in the western part of the Iberian Peninsula belong to the Silves Group that is considered the lower Mesozoic from the Lusitanian Basin and Algarve (e.g. Palain, 1976; Soares et al., 2012; Kullberg et al., 2013, and others). The Silves Group mainly consists of siliciclastic rocks. It is moderately well exposed in the Coimbra-Penela region, which is the focus of this work (Fig. 1). Several authors investigated the Silves Group in the LB (e.g. Carvalho, 1950; Palain, 1976, 1979). More recently, Soares et al. (2007, 2012) revised their stratigraphy and proposed a new lithostratigraphic chart: the Conraria, Penela, Castelo Viegas and Pereiros formations (Fig. 2). The Conraria Formation rests unconformably over late Precambrian or Carboniferous and is composed of ferruginous conglomerates and sandstones, attaining a maximum thickness of ~150 m in the Coimbra region. This formation is interpreted as alluvial plain deposits formed under an arid climate with intermittent short durations of intense precipitation (Palain, 1976; Soares et al., 2012). Plant fossils of



*Voltzia ribeiroi*, *Clathropteris* and *Otozamites* are typical of a Rhaetian age (Teixeira, 1942; Carvalho, 1950). However, recent palynological studies allowed the dating of the Conraria Formation as Norian, reaching possibly the early Rhaetian age (Vilas-Boas et al., 2021) (Fig. 2).

The Penela Formation consists of red and brownish sandy conglomerates with a thickness of 90–120 m in the Coimbra–Penela region (Soares et al., 2012). This unit is interpreted as deposited in a complex braided to meandering river system (Soares et al., 2012). The upper part of this unit, the Melhorado Beds (Soares et al., 2012), comprises brown/red sandy lutitic beds interpreted as overbank deposits with conspicuous calcite and dolomite nodules.

The Castelo Viegas Formation, about 110 m thick, consists of 4–5 m thick intervals of coarse-grained arkoses intercalated with centimetre thick lutitic. The unit is a coastal environment with arid paleoclimatic conditions (Palain, 1976; Soares et al., 2012).

Lastly, the Pereiros Formation marks a significant facies change; the basal part of the Pereiros Formation (B2 in Palain, 1976, 1979) is composed of fine crystalline dolostones with siliciclastics, alternating with millimetre to centimetre-thick mudstones, sometimes with pavements of bivalves (*Isocyprina*) and, very locally, of gastropods (*Promathildia*) (the *Isocyprina* Beds). This mixed carbonate-siliciclastic unit is about 6 m thick. It is followed upwards by a lenticular unit of coarse to very coarse brownish sandstones with rare plant fossils of the fern *Clathropteris meniscoides*, (the *Clathropteris* Beds, or unit C2 in Palain, 1976; see also Soares et al., 1993) (Teixeira, 1942; Kullberg et al., 2013). The upper part of the Pereiros Formation consists of reddish and greyish sandy lutites with fine-grained dolomites and dolomitic marls with patchy gypsum lenses; this is the thickest and lithologically most complex subunit of the Pereiros Formation (Azerêdo et al., 2003; Sêco et al., 2015). This unit was deposited in an evaporitic environment of shallow lagoons, changing to lagoonal settings delimited by sandy barrier islands and culminated at the top with laminated dolostones (Curtis et al., 1963; Shinn, 1983; Mazzullo, 2000; Soares et al., 2012). The Coimbra Formation overlaps the Pereiros Formation (Dimuccio et al., 2014, 2016; Gomez et al., 2019; Duarte et al., 2022). The invertebrate fauna and plant fossils in the Pereiros Formation indicate a Hettangian age

(Teixeira, 1942). However, recent palynological studies date the entire Pereiros Formation as late Rhaetian to early Hettangian (Vilas-Boas et al., 2021).

## MATERIALS AND METHODS

### STUDIED SECTIONS: STRATIGRAPHY AND GENERAL DESCRIPTIONS

The Pereiros Formation was sampled in the Lamas I (coordinates: 40°4'44.35"N; 8°22'48.30"W) and Lamas II (coordinates: 40°5'6.42"N; 8°23'10.30"W) (LAMAS and LAM, respectively) sections located at Lamas, Miranda do Corvo region (Figs 1 and 3).

From the Lamas I section, 19 samples were collected, 15 yielded sporomorphs, and four were barren (Fig. 4; Table 1). The samples from this section were collected from the lowermost part of the Pereiros Formation (unit B2 in Palain, 1976), consisting of shallow marine carbonate-siliciclastic intervals.

The Lamas II section is the reference section of unit C2 of the Pereiros Formation; from the 12 samples collected, 10 yielded sporomorphs, and two were barren (Fig. 4; Table 1). The lower part of this section consists of argillaceous sandstones sometimes intercalated with metre-thick sandy dolostones, and the upper part consists of dolomitic marls and dolostones. The top of this section marks the contact between the Pereiros and Coimbra formations. The lowermost part of the Coimbra Formation comprises thin (centimetre-scale) intercalations of bedded grey marls and metre-scale dolostones.

### PALYNOSTRATIGRAPHIC AND PALYNOFACIES TECHNIQUES

Thirty-one lutitic samples were collected from two sections in the Coimbra region (see Figs 1–3 for the locations of the sections sampled). Palynostratigraphic and palynofacies analyses were carried out in all collected samples. The samples were processed at the Portuguese Geological Survey (LNEG) and Centre for Marine and Environmental Research, University of Algarve (CIMA-UAIG) using standard palynological laboratory procedures in the extraction (treated with hydrochloric and hydrofluoric acids) of the organic residue following the methodologies described by Wood et al. (1996) and Riding and Warny (2008). The organic residues were not oxidised. The organic residues were sieved using a 15 µm sieve and then mounted on microscope slides using Entelan®, a commercial resin-based mounting medium. The slides were used in palynostratigraphic and palynofacies studies.

The slides for the palynostratigraphic study were analysed using a Leica DM750 microscope equipped with a Leica ICC50W camera. In the 25 palynological productive samples, semi-quantitative abundance was determined by counting 350 specimens per slide whenever possible. The slides were also scanned for rare taxa, which were recorded as present outside the count (see Table 1, signed with an X). The counts per sample and taxa are listed in Table 1. The quantitative data

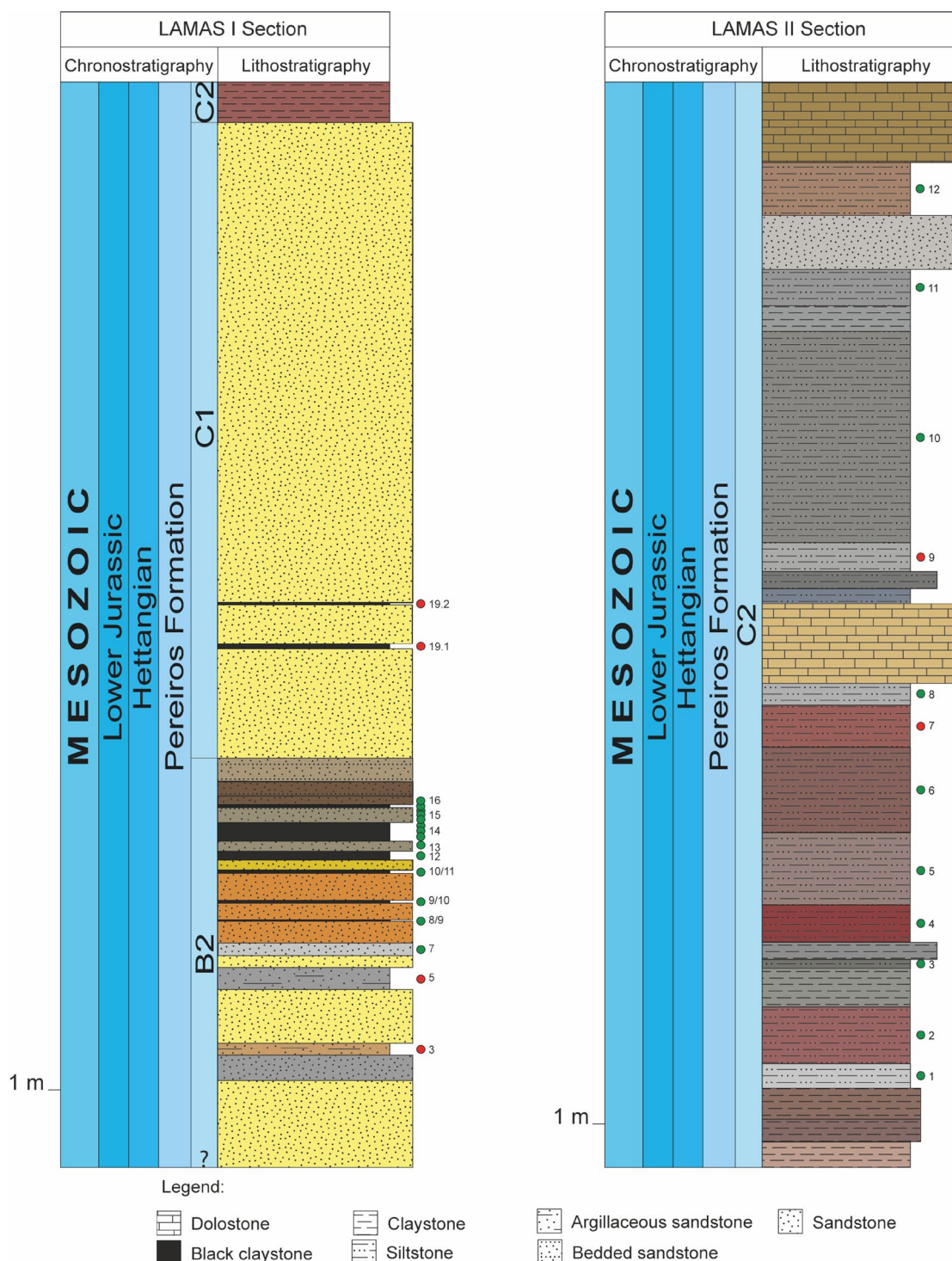


**Figure 3.** Stratigraphic Log of Lamas I and Lamas II. Dots in the logs mark the location of the studied samples. Green dots point out productive samples for palynological studies, and red dots point out barren samples for palynological studies. The colours used in the stratigraphic logs are intended to represent the shades observed in each layer in the field

were described as follows: rare (0–10%), common (11–50%) and abundant (>51%). Stratigraphical relevant taxa are presented on Figures 5 and 6.

A quantitative approach was used for all 31 samples studied with palynofacies analyses. Three hundred and fifty organic particles were counted in each slide using Olympus BX51 equipped with an Olympus XC-50 digital camera. An adapted scheme from Tyson (1993, 1995) was used for palynofacies interpretation. Absolute and relative counts for all samples are presented

in Table 3. Table 2 illustrates the different palynofacies groups identified in this study. Representative palynofacies are shown in Figure 7. All samples, residues and slides are currently curated at the University of Algarve and the Palynological Collection of LNEG, Portugal. All palynostratigraphic and palynofacies results are plotted in Figs 4 and 8 using Tilia 3.0.1 software (Grimm, 1991).

The paleoenvironmental interpretation is based on the relative abundances of specific palynomorph groups and palynofacies integrated with lithofacies.

**Table 1.** Dataset (%) for terrestrial palynomorphs (spores and pollen grains) and marine palynomorphs (foraminiferal linings). Relative abundance. X – Registered outside the count. SP/F Ratio – Sporomorphs (spores + pollen grains)/Foraminiferal lining.

Outcrops	LAMAS I														
	LAMAS 7	LAMAS 8/9	LAMAS 9/10	LAMAS 10/11	LAMAS 12	LAMAS 13	LAMAS 14BASE	LAMAS 14INT	LAMAS 14TOPO	LAMAS 15a) BASE	LAMAS 15b) BASE	LAMAS 15INT	LAMAS 15 TOPO	LAMAS 15/16	LAMAS 16
Samples															
SPORES															
<i>Apiculatisporis</i> sp.		0.8		0.3											
<i>Calamospora tener</i> (Leschik 1955) Mädler 1964		0.8		0.3	X		X	1.2	0.4	0.4	0.4	0.4	0.4		
<i>Carnisporites</i> sp.									1.2			3.6	1.6		X
<i>Carnisporites spiniger</i> (Leschik) Morbey 1975		5.2	7.5		16	10.4	13.6	12.4	15.2	14.3	17.2	6	6.8	13.2	7.6
<i>Cibotiumspora</i> sp.		0.8	0.4	0.9	0.4	X	X	1.2	0.4	0.4		X	X		1.6
<i>Converrucosporites</i> sp.								0.4							
<i>Convolutispora</i> sp.									X	0.4	X	0.4	1.6		0.4
<i>Cyathidites</i> sp.		12	7.9	10	6.8	4	2	2.8	4.8	5.6	5.2	4.8	5.2	5.2	9.6
<i>Deltoidospora halli</i> Miner 1935								0.4							
<i>Deltoidospora</i> sp.		18.8	27.7	9.1	5.6	9.2	10.4	13.6	16.8	18.3	13.2	15.1	16.8	18	19.2
<i>Dictyophyllidites mortonii</i> (de Jersey) Playford et Dettman 1965						0.4				0.4	0.8	X		1.2	3.2
<i>Dictyophyllidites</i> sp.								1.6	2	2.8	3.6	2	2.4	0.8	4.8
<i>Foveosporites foveoreticulatus</i> Dring 1965							0.8								
<i>Foveosporites</i> sp.		0.8						2.4						1.2	
<i>Ischyosporites</i> sp.											1.6	X			0.8
<i>Ischyosporites variegatus</i> (Couper 1958 ) Schulz 1967				1.1	X	0.8	X	0.8	0.4	0.4	1.2			2	
<i>Kraeuselisporites reissingeri</i> (Harris 1957) Morbey 1975	100	19.6	38.3	15.4	28	26.8	23.6	29.2	24.8	27.5	18.8	21.9	25.6	28.4	20
<i>Kraeuselisporites</i> sp.				1.1	0.8										
<i>Kyrtomispors</i> sp.		0.8		0.9	0.4	0.8	2			0.8					
<i>Leiotriletes directus</i> Balme et Hennelly 1956					14										
<i>Leptolepidites</i> sp.														X	2.4
<i>Polypodiisporites</i> sp.		0.4													
<i>Porcellispora longdonensis</i> (Clarke) Scheuring emend. Morbey 1975						0.4			X					X	
<i>Retitriletes austracalvatidites</i> (Cookson) Döring et al. 1963									0.4						
<i>Todisporites</i> sp.				11.1						2	1.6	1.2	2.4		
<i>Trachysporites fuscus</i> Nilsson 1958														0.4	
<i>Trachysporites</i> sp.		0.4												0.4	8.4
<i>Uvaesporites</i> sp.				0.3											
Sum Spores	100	60.4	81.8	50.5	72	52.8	52.4	66	66.4	73.3	63.6	55.4	62.8	70.8	78
POLLEN															
<i>Alisporites</i> sp.						0.4									
<i>Araucariacites</i> sp.															
<i>Chasmatosporites</i> sp.															
<i>Classopollis</i> abnormal							X	X	0.4				3.2	1.6	X
<i>Classopollis meyerianus</i> (Klaus) de Jersey 1973		33.6	7.9	31.4	23.6	37.2	45.2	30.8	32.4	26.3	33.6	43.8	32.8	23.2	16.8
<i>Classopollis</i> sp.		2.4	0.4	2		3.2									0.4
<i>Classopollis torosus</i> Reissinger 1950			7.5	11.4	3.2	2									
<i>Cycadopites</i> sp.					X		0.8	1.2							
<i>Inaperturopollenites</i> sp.															
<i>Paracirculina</i> sp.				4											
<i>Perinopollenites elatoides</i> Couper 1958				0.6	1.2	1.6		X		0.4	0.4	0.4		0.8	
<i>Pinuspollenites minimus</i> (Couper) Kemp 1970		2.8	1.6		X	1.6	1.6	1.2	0.4		2	0.4	0.4	3.6	4
Sum Pollen	0	38.8	17.4	49.4	28	46	47.6	33.2	33.2	26.7	36	44.6	36.4	29.2	21.2
Foraminiferal lining		0.8	0.8			1.2	X	0.8	0.4		0.4		0.8		0.8
SP/F Ratio		0.992	0.992			0.988		0.992	0.996		0.996		0.992		0.992

Table 1. Continued

[illegible]



## RESULTS

## PALYNOFACIES

The studied sections allowed the retrieval of 29 productive palynofacies samples representing the three units from the Pereiros Formation, B2, C1 and C2 (Palain, 1976, 1979) (Tables 2, 3; Fig. 7).

## Unit B2

Seventeen samples were collected from this unit, and fifteen were productive for palynofacies analyses. The phytoclast group is dominant in all the 15 samples (average 76.1%; Table 3). The non-opaque subgroup is the most representative of the phytoclast group with an average abundance of 61.5%, achieving the lowest percentage of 46.3% at ~2.8 m (LAMAS 7) and the highest percentage value of 79.7% at ~3.2 m (LAMAS 8/9) (Table 3; Fig. 8). The relative abundance of opaque phytoclasts is 14.5% and reaches a peak of 42.3% at ~2.8 m (LAMAS 7) and a minimum of 1% at ~4.5 m (LAMAS 14 INT) (Table 3; Figs 7, 8). The percentage of the terrestrial palynomorphs (spores and pollen) is consistent over the entire outcrop, with the spores dominating the pollen with an average percentage of 9.6% and 7.8%, respectively. The foraminifera linings are recorded at ~3.2 m and 4.5 m (LAMAS 15TOPO), with a relative abundance of 0.3% in both samples; however, they are present in most of the samples from this unit. A relative abundance of 0.7% of amorphous organic matter (AOM) is identified; the subgroup with fluorescence is only recognised at ~2.8 and 4.2 m (LAMAS 13) with a value of 0.3%, and the subgroup with no fluorescence ranges from 0.3% at ~4.5 m to 3.3% to ~4.6 m

(LAMAS 15a) BASE). In addition, a relative abundance of the vegetal particle group, ranging from 0.3% at ~3.9 m (LAMAS 10/11) to 7.7% at ~4.5 m (LAMAS 14TOPO) with fluorescence and ranging from 0.3% at 3.9 m to 9.3 % ~4.5 m (LAMAS 14BASE) is identified (Table 3; Fig. 7).

## Unit C1

From unit C1, two samples were collected. Both were productive for palynofacies analyses, although only phytoclasts were present (Table 3). The non-opaque subgroup is the most representative of the phytoclast group with an average abundance of 70.5%, achieving the lowest percentage of 51.3% at ~7.3 m (LAMAS 19.2INT) and the highest percentage value of 89.7% at ~6.8 m (LAMAS 19.1BASE) (Table 3; Fig. 8). The relative abundance of opaque phytoclasts is 29.5% and reaching a peak of 48.7% at 6.8 m and a minimum of 10.3% at ~7.3 m (Table 3; Fig. 8). The samples were barren for vegetal particles, AOM and palynomorphs (e.g. spores, pollen grains, foraminiferal linings).

## Unit C2

In this unit, all the twelve samples analysed were productive. The phytoclast group is dominant in all the samples (average 57.9%; Table 3; Fig. 8) except for ~16.2 m (LAM 10) and ~19.9 m (LAM 11). The non-opaque subgroup is the most representative of the phytoclast group with an average abundance of 30.7%, achieving the lowest percentage of 4% at ~19.9 m and the highest percentage of 60% at ~4.8 m (LAM 3) (Table 3). The relative abundance of opaque phytoclasts is 27.2%,

**Table 2.** Description of palynofacies groups used in this study (based on Tyson, 1993, 1995)

Palynomorphs	Spores	The cell that certain plants (such as Filicopsids, Sphenophytes, Lycophytes, and Bryophytes) produce and use to reproduce. Consisting of monolete, trilete and alele spores.	
	Pollen	The cell that Gymnosperms and Higher Seed Ferns use to reproduce.	
	Foraminiferal lining	The preserved internal organic remains of Microforaminifera. The presence of foraminiferal linings indicates marine influence.	
Phytoclasts	Organic material derived from the ligno-cellulosic tissues of terrestrial macrophytes	Non-opaque	Ligno-cellulosic tissue that under the microscopy light are non-opaque or translucent.
		Opaque	Ligno-cellulosic tissue that have no visible structure and appear to be homogeneous. Under the light of the microscopy appears completely black (opaque).
		Vegetal Particles	Tissue of probable plant origin.
Amorphous Organic Matter		Includes phytoplankton- or bacterially derived amorphous organic matter and amorphous products of the diagenesis of macrophyte tissues that under the light of the microscope appears structureless. The preservation of AOM indicates dysoxic or anoxic conditions.	



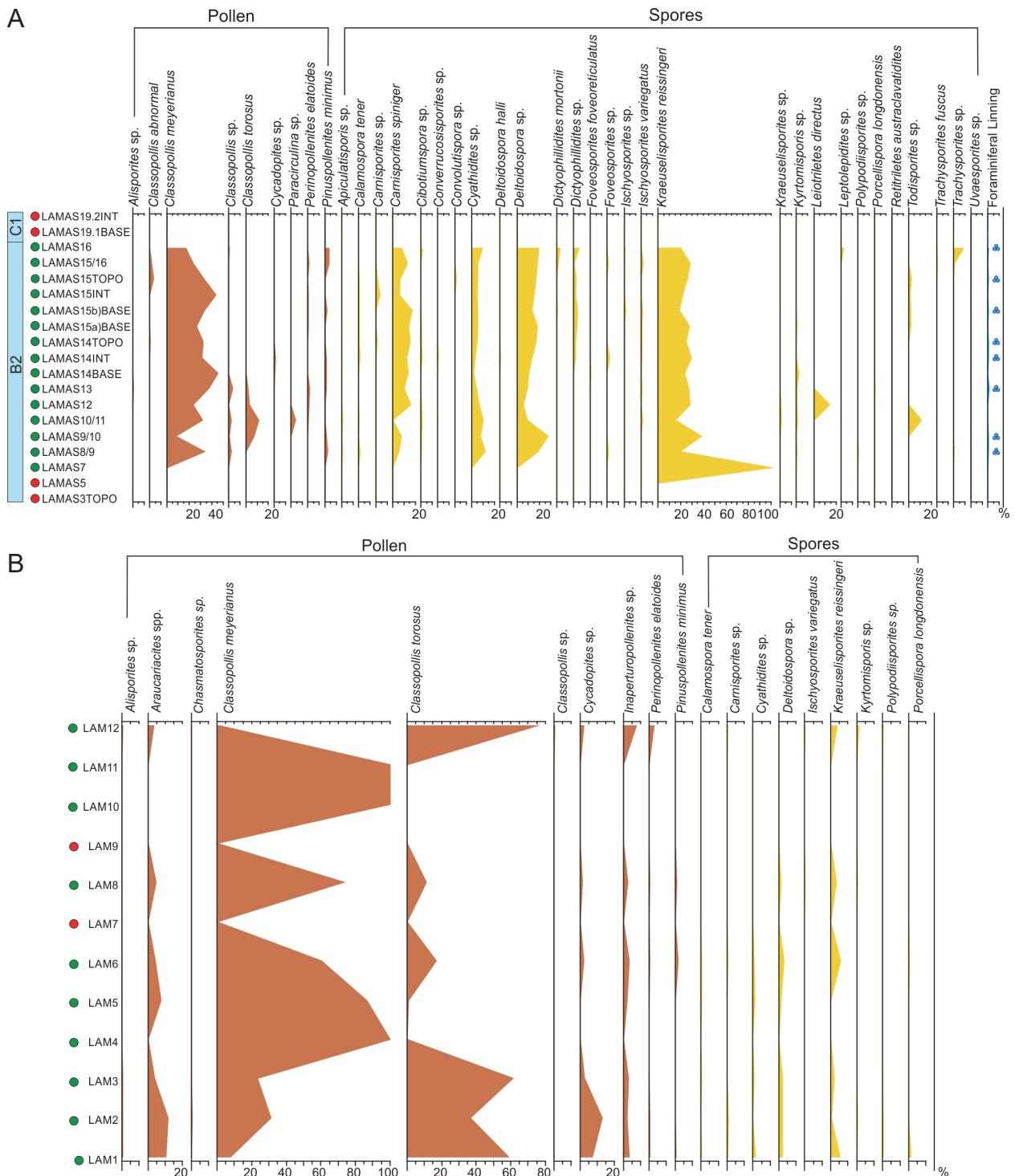


**Figure 4.** Composite range chart of the sporomorph taxa found in the studied sections. **A.** Range chart of Lamas I outcrop. The blue symbol marks the samples that contain foraminifera linings; **B.** Range chart of Lamas II. Green dots indicate productive samples for palynological studies, and red dots indicate barren samples for palynological studies. Not to scale

reaching a peak of 85.7% at ~13.5 m (LAM 9) and a minimum of 1.3% at ~16.2 m (Table 3). The pollen subgroup dominates the group of the sporomorphs, in all the samples, with an average percentage of 32.4% to an average percentage of 0.3 % for the spore subgroup. A relative abundance of the AOM is identified, the subset fluorescent varies from a value of 0.3%

at ~4.8, 10 (LAM 7), and 19.9 m to a value of 5% at ~22 m (LAM 12) and the subgroup with no fluorescence ranges from 0.3% at ~2.9 (LAM 2), 4.8, 10.5 (LAM 8; Fig. 7), 13.5 and 16.2 m to 1.3% at ~8.5 (LAM 6) and 10 m.

In addition, a relative abundance of the vegetal particle group has been recorded, ranging from 0.3% at ~19.9 m to 29.5% at ~6.8 m

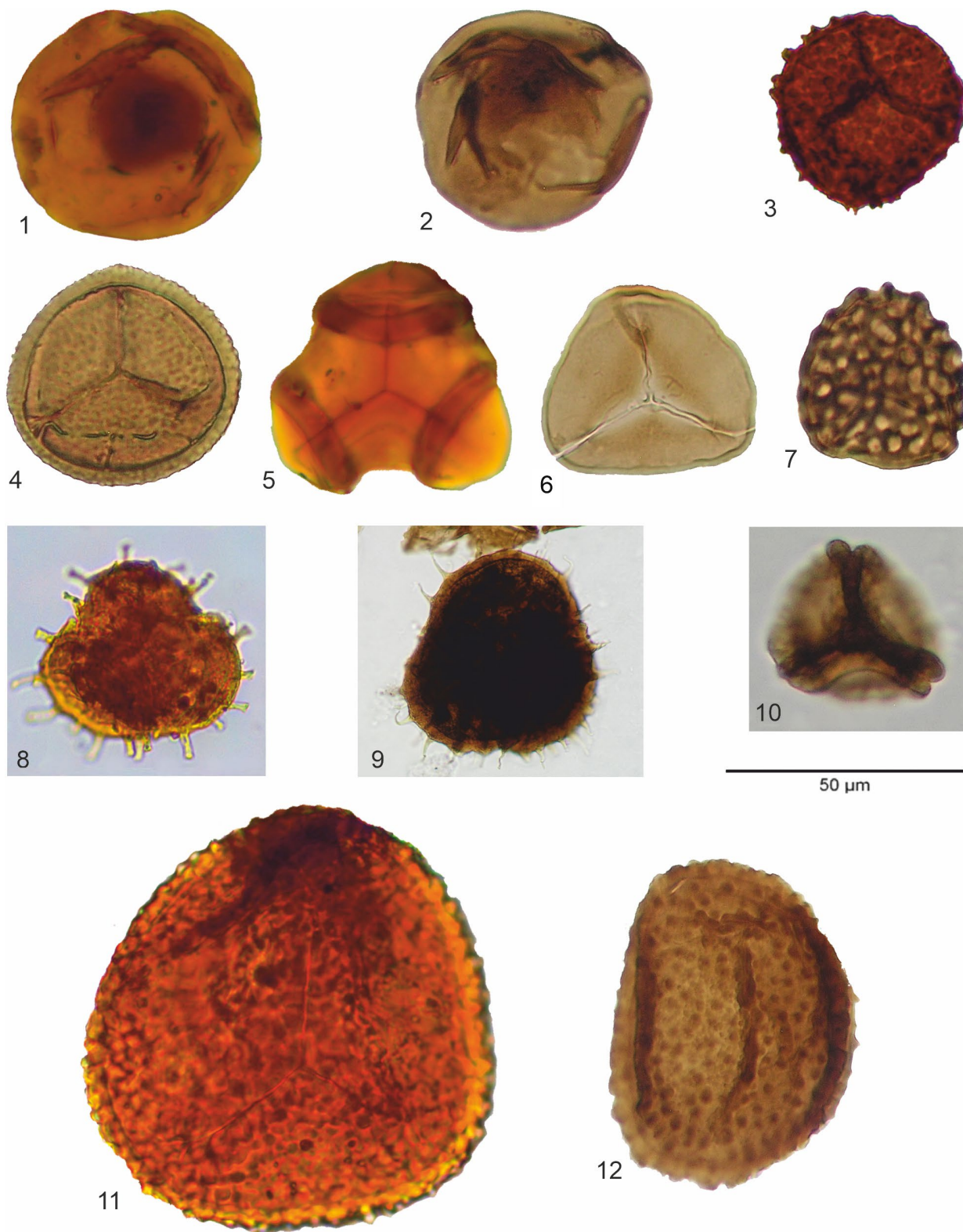


**Figure 5.** Selected spores from Lamas I and Lamas II sections. The species name is followed by the outcrop, sample, slide number, and microscope coordinates. 1. *Calamospora tener* (Leschik) Mädlar 1964, Outcrop Lamas I; sample LAMAS 14INT; slide 1 (1202-205); 2. *Calamospora tener* (Leschik) Mädlar 1964, Outcrop Lamas II; sample LAM 1; slide 2 (1130-115); 3. *Carnisporites spiniger* (Leschile) Morbey 1975, Outcrop Lamas I, sample LAMAS 8/9; slide 1 (1309-105); 4. *Carnisporites* sp., Outcrop Lamas II; sample LAM 1; slide 8 (1440-205); 5. *Cibotiumspora* sp., Outcrop Lamas I; sample LAMAS 10/11; slide 1 (1281-209); 6. *Deltoidospora* sp., Outcrop Lamas II, sample LAM 5; slide 1 (1355-125); 7. *Ischyosporites variegatus* (Couper) Schulz 1967, Outcrop Lamas II, sample LAM 12; slide 3 (1305-205); 8. *Kraeuselisporites reissingeri* Leschik emend. Jansonius 1962, Outcrop Lamas I; sample LAMAS 13; slide 1 (1240-60); 9. *Kraeuselisporites reissingeri* Leschik emend. Jansonius 1962, Outcrop Lamas II; sample LAM 12; slide 1 (1387-175); 10. *Kyrtoisporis* sp., Outcrop Lamas II; sample LAM 12; slide 1 (1395-71); 11. *Convolutispora* sp., Outcrop Lamas I; sample LAMAS 12; slide 1 (1205-161); 12. *Porcellispora longdonensis* (Clarke) Scheuring emend. Morbey 1975, Outcrop Lamas II; sample LAM 1; slide 8 (1200-125)



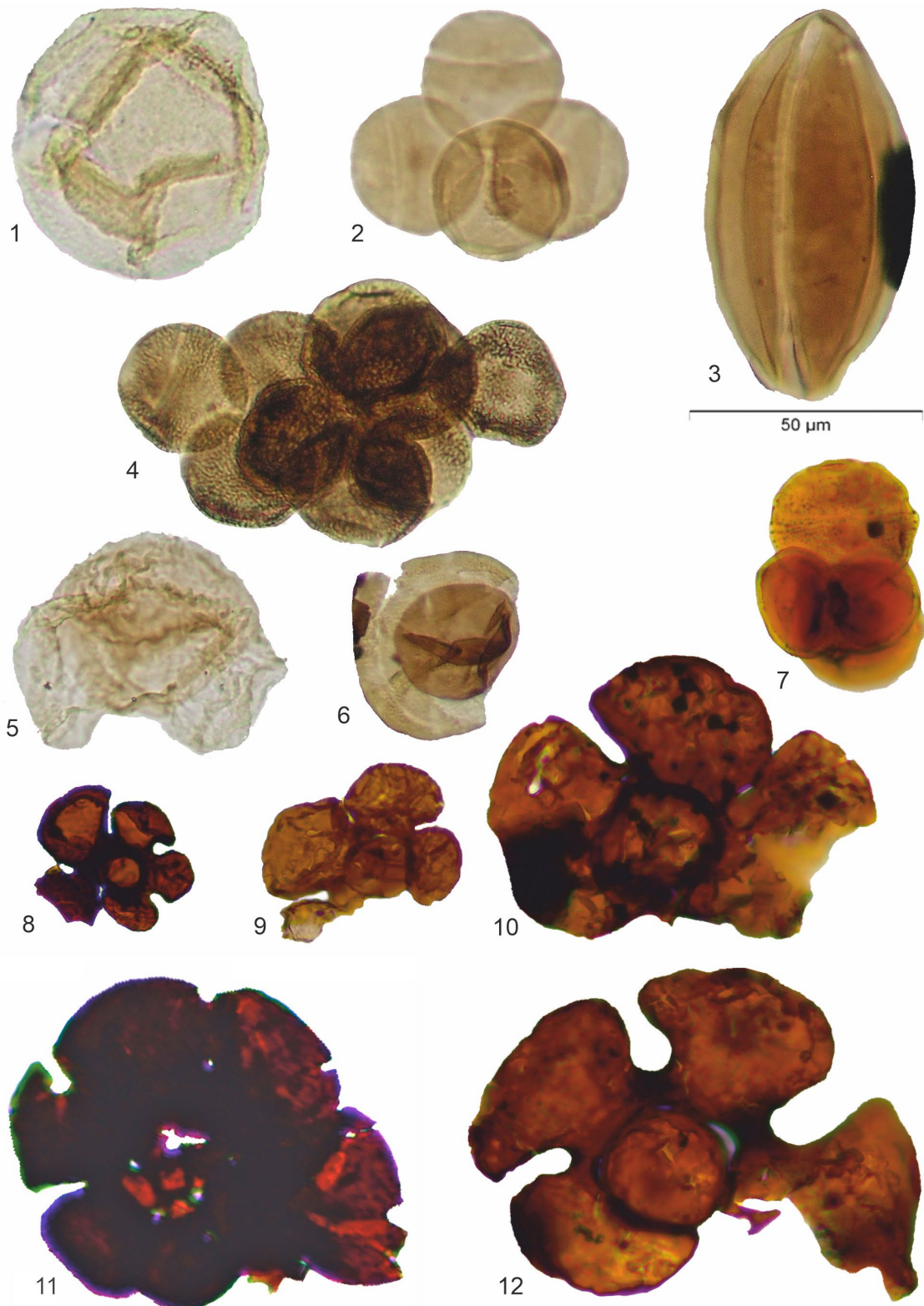


**Figure 6.** Selected pollen and foraminifera lining from Lamas I and Lamas II sections. The species name is followed by the outcrop, sample, slide number, and microscope coordinates. 1. *Araucariacites* sp., Outcrop Lamas II; sample LAM 1; slide 2 (1145-184); 2. *Classopollis meyerianus* (Klaus) Venkatachala et Góczán 1964, Outcrop Lamas II; sample LAM 2; slide 5 (1340-25); 3. *Cycadopites* sp., Outcrop Lamas II; sample LAM 2; slide 1 (1225-95); 4. *Classopollis torosus* (Reissinger) Klaus emend. Cornet et Traverse 1975, Outcrop Lamas II; sample LAM 1; slide 2 (1430-150); 5. *Pinuspollenites minimus* (Couper) Kemp 1970, Outcrop Lamas II; sample LAM 6; slide 2 (1415-268); 6. *Perinopollenites elatoides* Couper 1958, Outcrop Lamas II; sample LAM 12; slide 4 (1055-117); 7. *Classopollis meyerianus* with abnormal pollen of *Classopollis* (Klaus) Venkatachala et Góczán 1964, Outcrop Lamas I, sample LAMAS 14INT; slide 1 (1212-205); 8. Foraminiferal lining, Outcrop Lamas I, sample LAMAS 13; slide 1 (1250-150); 9. Foraminiferal lining, Outcrop Lamas I, sample LAMAS 8/9; slide 1 (1381-112); 10. Foraminiferal lining, Outcrop Lamas I, sample LAMAS 10/11; slide 1 (1203-90); 11. Foraminiferal lining, Outcrop Lamas I, sample LAMAS 13; slide 1 (1385-110); 12. Foraminiferal lining, Outcrop Lamas I, sample LAMAS 10/11; slide 1 (1201-171)



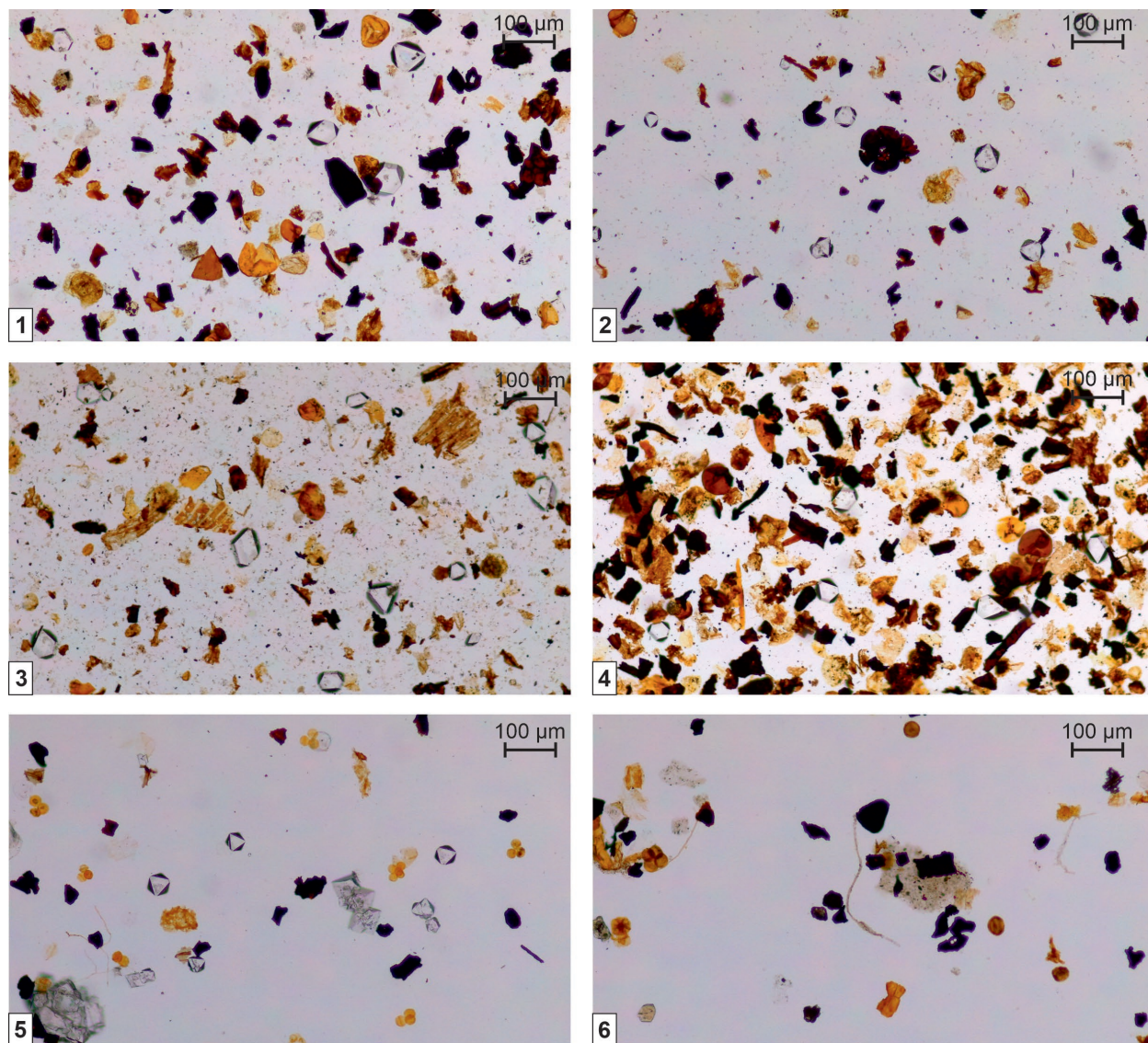


**Figure 7.** Selected palynofacies assemblages from the outcrops Lamas I and Lamas II. 1. Dominance of phytoclasts opaque and non-opaque and spores from the Lamas I outcrop, sample LAMAS 12; 2. Presence of foraminiferal lining from the Lamas I outcrop, sample LAMAS 13; 3. Dominance of non-opaque phytoclasts from the Lamas I outcrop, sample LAMAS 14BASE; 4. Dominance of phytoclasts opaque and non-opaque and spores from the Lamas I outcrop, sample LAMAS 14INT; 5. Presence of more common *Classopollis* spp. pollen grains in tetrads from the Lamas II outcrop, sample LAM 8; 6. Dominance of pollen grains and opaque phytoclasts from the Lamas II outcrop, sample LAM 12

(LAM 5) with an average percentage of 6.8% for the fluorescent subgroup and ranging from 0.3% at ~5.5 (LAM 4), 10.5 and 16.2 m to 3.9% at ~2.9 m with an average of 1.3% for the non-fluorescent subgroup (Table 3).

#### PALYNOLOGICAL ASSEMBLAGES

##### Unit B2

Unit B2 presents 21 and 6 moderately to well-preserved species of spores and pollen grains, respectively (Table 1; Figs 4–6). This unit is characterised by the presence of *Kraeuselisporites reissingeri* and *Ischyosporites variegatus*, together with some other spores,

such as common to abundant *Carnisporites spiniger*, *Cyathidites* sp., *Deltoidospora* sp., and rare *Calamospora tener*, *Dictyophyllidites mortonii*, *Dictyophyllidites* sp., *Porcellispora longdonensis*, *Todisporites* sp., *Trachysporites fuscus* and *Trachysporites* sp. *Dictyophyllidites mortonii* makes its last occurrence (LO) in the sample LAMAS16, ~4.8 m in the section. The association is completed with common to abundant pollen grains of *Classopollis meyerianus* with rare to common *Classopollis torosus* and rare *Alisporites* sp., *Cycadopites* sp., *Perinopollenites elatoides*, *Pinuspollenites minimus*. In this unit, well to moderately preserved foraminifera linings are notable in 9 of the 19 samples collected (Table 1).

**Table 3.** Quantitative analysis, percentage data presented per sample and group for the palynofacies analyses. AOM – Amorphous organic matter; FL – Foraminiferal lining; Op. – Opaque; Fluo. – Fluorescence

Outcrop LAMAS I / Samples		Palynomorphs				Phytoclasts			Vegetal Particles			AOM			Total
		Spores	Pollen	FL	Total	Op.	Non-op.	Total	With Fluo.	No Fluo.	Total	With Fluo.	No Fluo.	Total	
LAMAS 19.2INT	Count	0	0	0	0	146	154	300	0	0	0	0	0	0	300
	%	0	0	0	0	48.7	51.3	100	0	0	0	0	0	0	100
LAMAS 19.1BASE	Count	0	0	0	0	31	269	300	0	0	0	0	0	0	300
	%	0	0	0	0	10.3	89.7	100	0	0	0	0	0	0	100
LAMAS 16	Count	16	15	0	31	113	157	270	4	0	4	0	0	0	305
	%	5.2	4.9	0	10.1	37	51.5	88.5	1.3	0	1.3	0	0	0	100
LAMAS 15/16	Count	43	24	0	67	47	186	233	0	0	0	0	0	0	300
	%	14.3	8	0	22.3	15.7	62	77.7	0	0	0	0	0	0	100
LAMAS 15TOPO	Count	22	24	1	47	57	208	265	0	2	2	0	1	1	315
	%	7	7.6	0.3	14.9	18.1	66	84.1	0	0.6	0.6	0	0.3	0.3	100
LAMAS 15INT	Count	19	41	0	60	121	165	286	0	0	0	0	0	0	346
	%	5.5	11.8	0	17.3	35	47.7	82.7	0	0	0	0	0	0	100
LAMAS 15b) BASE	Count	16	38	0	54	8	241	249	0	0	0	0	0	0	303
	%	5.3	12.5	0	17.8	2.6	79.5	82.1	0	0	0	0	0	0	100
LAMAS 15a) BASE	Count	27	33	0	60	9	211	220	7	3	10	0	10	10	300
	%	9	11	0	20	3	70.3	73.3	2.3	1	3.3	0	3.3	3.3	100
LAMAS 14TOPO	Count	47	33	0	80	9	169	178	23	16	39	0	3	3	300
	%	15.7	11	0	26.7	3	56.3	59.3	7.7	5.3	13	0	1	1	100
LAMAS 14INT	Count	37	26	0	63	3	224	227	6	4	10	0	0	0	300
	%	12.3	8.7	0	21	1	74.7	75.7	2	1.3	3.3	0	0	0	100
LAMAS 14BASE	Count	18	39	0	57	16	184	200	14	28	42	0	1	1	300
	%	6	13	0	19	5.3	61.3	66.6	4.7	9.3	14	0	0.3	0.3	100
LAMAS 13	Count	20	40	0	60	37	166	203	15	14	29	1	7	8	300
	%	6.7	13.3	0	20	12.3	55.3	67.6	5	4.7	9.7	0.3	2.3	2.6	100
LAMAS 12	Count	83	23	0	106	27	167	194	0	0	0	0	0	0	300
	%	27.7	7.7	0	35.4	9	55.7	64.7	0	0	0	0	0	0	100
LAMAS 10/11	Count	65	31	0	96	32	190	222	1	1	2	0	0	0	320
	%	20.3	9.7	0	30	10	59.4	69.4	0.3	0.3	0.6	0	0	0	100
LAMAS 9/10	Count	56	18	0	74	57	183	240	0	0	0	0	4	4	318
	%	17.6	5.7	0	23.3	17.9	57.5	75.4	0	0	0	0	1.3	1.3	100
LAMAS 8/9	Count	8	24	1	33	18	239	257	3	2	5	0	5	5	300
	%	2.7	8	0.3	11	6	79.7	85.7	1	0.7	1.7	0	1.7	1.7	100
LAMAS 7	Count	25	0	0	25	127	139	266	3	2	5	1	3	4	300
	%	8.3	0	0	8.3	42.3	46.3	88.6	1	0.7	1.7	0.3	1	1.3	100
Outcrop LAMAS II / Samples															
LAM 12	Count	3	88	0	91	90	66	156	33	6	39	15	2	17	303
	%	1	29	0	30	29.7	21.8	51.5	10.9	2	12.9	5	0.7	5.7	100
LAM 11	Count	0	277	0	277	7	12	19	1	0	1	1	2	3	300
	%	0	92.3	0	92.3	2.3	4	6.3	0.3	0	0.3	0.3	0.7	1	100
LAM 10	Count	0	279	0	279	4	29	33	3	1	4	3	1	4	320
	%	0	87.2	0	87.2	1.3	9.1	10.4	0.9	0.3	1.2	0.9	0.3	1.2	100
LAM 9	Count	0	0	0	0	257	36	293	6	0	6	0	1	1	300
	%	0	0	0	0	85.7	12	97.7	2	0	2	0	0.3	0.3	100
LAM 8	Count	1	142	0	143	106	45	151	2	1	3	2	1	3	300
	%	0.3	47.3	0	47.6	35.3	15	50.3	0.7	0.3	1	0.7	0.3	1	100
LAM 7	Count	0	0	0	0	156	89	245	41	9	50	1	4	5	300
	%	0	0	0	0	52	29.7	81.7	13.7	3	16.7	0.3	1.3	1.6	100
LAM 6	Count	0	83	0	83	61	129	190	17	6	23	0	4	4	300
	%	0	27.7	0	27.7	20.3	43	63.3	5.7	2	7.7	0	1.3	1.3	100
LAM 5	Count	3	43	0	46	64	93	157	89	5	94	3	2	5	302
	%	1	14.2	0	15.2	21.2	30.8	52	29.5	1.7	31.2	1	0.7	1.7	100
LAM 4	Count	1	13	0	14	165	119	284	4	1	5	0	0	0	303
	%	0.3	4.3	0	4.6	54.5	39.3	93.8	1.3	0.3	1.6	0	0	0	100
LAM 3	Count	4	65	0	69	15	180	195	29	5	34	1	1	2	300
	%	1.3	21.7	0	23	5	60	65	9.7	1.7	11.4	0.3	0.3	0.6	100
LAM 2	Count	0	87	0	87	30	166	196	10	12	22	0	1	1	306
	%	0	28.4	0	28.4	9.8	54.2	64	3.3	3.9	7.2	0	0.3	0.3	100
LAM 1	Count	0	109	0	109	28	149	177	10	2	12	2	0	2	300
	%	0	36.3	0	36.3	9.3	49.7	59	3.3	0.7	4	0.7	0	0.7	100



## Unit C2

The palynological assemblage recovered in unit C2 includes well-preserved spores (nine species) and pollen grains (eight species) (Table 1; Figs 4–6). The spores include *Calamospora tener*, *Ischyosporites variegatus* and *Kraeuselisporites reissingeri*. The association is completed with the spores of *Carnisporites* sp., *Cyathidites* sp., *Deltoidospora* sp., *Kyrto-misporis* sp., *Polypodiisporites* sp. and *Porcellispora longdonensis*. *Classopollis meyerianus* and *Classopollis torosus* are common to abundant, while *Alisporites* sp., *Araucariacites* sp., *Cycadopites* sp., *Inaperturopollenites* sp., *Perinopollenites elatoides* are rare to common. The spores of *Pinuspollenites minimus* are also present.

## DISCUSSION

## AGE OF THE PEREIROs FORMATION

Palynostratigraphic studies carried out previously in the Triassic–Jurassic Silves Group are relatively limited. The first investigations were carried out by Doubinger et al. (1970), continued by Adloff et al. (1974), based on the sedimentological and allostratigraphical work of Palain, who divided the Silves Group into three megasequences A, B and C (Palain, 1976, 1979). Díez (2000) studied the same associations and concluded that the Conraria Formation [Megasequence A from Palain (1976)] dates from the lower to middle Carnian and includes the taxa *Classopollis meyerianus*, *Duplicisporites granulatus*, *D. mancus*, *Microcachrydites doubingeri*, *M. fastidioides*, *Monosulcites minimus*, *Ovalipollis cultus*, *Paracirculina scurrilis* and *P. maljawkinae*. The Penela and Castelo Viegas formations [Megasequence B from Palain (1976)] show palynological associations (Adloff et al., 1974) that include *Araucariacites germanicus*, *Classopollis granulatus*, *C. meyerianus*, *Duplicisporites granulatus*, *Ischyosporites mesofoveosolidus*, *Kraeuselisporites reissingeri*, *Paracirculina tenebrosa* and *Todisporites major*, suggesting an age from middle Carnian to latest Norian (Díez, 2000; Arche and López-Gómez, 2014). The Pereiros Formation [Megasequence C, Term C1 from Palain (1976)] has an association comprising taxa such as *Classopollis clas-soides*, *Cycadopites granulatus*, *C. deterius*,

*Inaperturopollenites dubius* and *Kraeuselisporites reissingeri*, among others, and was considered of Hettangian to Sinemurian age since Adloff et al. (1974). Based on the common presence of the taxa *Kraeuselisporites reissingeri*, Díez (2000) and Arche and López-Gómez (2014) propose a Norian to lower Rhaetian age for the C1 term.

However, type-sections of the Silves Group have recently been investigated, and the results suggest different ages for these formations (Vilas-Boas et al., 2021). Based on palynostratigraphic studies, Vilas Boas et al. (2021) dates the Conraria Formation to Norian, possibly early Rhaetian and the Pereiros Formation to late Rhaetian – early Hettangian, suggesting that the TJB should lie in the lowermost Pereiros Formation.

Therefore, an early Hettangian age could be suggested for the unit B2 studied in this work. In the previous study, the lower portion of the Pereiros Formation (unit B2 in Palain, 1976; Lamas I) was dated to Rhaetian up to the TJB based on the informal palynozone *Ischyosporites variegatus-Kraeuselisporites reissingeri* (IK), while the mid-upper portion (units C1 and C2 in Palain, 1976; Lamas II) was dated to early Hettangian based on the informal palynozone *Pinuspollenites minimus* (Pm) (Vilas-Boas et al., 2021). An important discontinuity in the lowermost portion of the Pereiros Formation truncates the siliciclastic beds at the top of the Castelo Viegas Formation (Fig. 2), which has been regarded as the regional mapping boundary between the Triassic and Jurassic (Soares et al., 2007, 2012). However, the palynological evidence supports a position of the TJB within unit B2 at the base of the Pereiros Formation (Vilas-Boas et al., 2021). In this new study, it is worth noting that *Carnisporites spiniger* is present in unit B2. This spore is very common through most of the samples in this unit, ranging from the Anisian, Middle Triassic, where this spore has its first occurrence, and being consistent through the entire Upper Triassic (Vigran et al., 2014; Paterson and Mangerud, 2020).

Based on the presence of *Pinuspollenites minimus*, *Perinopollenites elatoides* and the dominance of *Classopollis meyerianus*, these sections date to the Hettangian, being the base of unit B2 from the base of the Hettangian.

However, the presence of *P. longdonensis* can also support a Hettangian age. The first



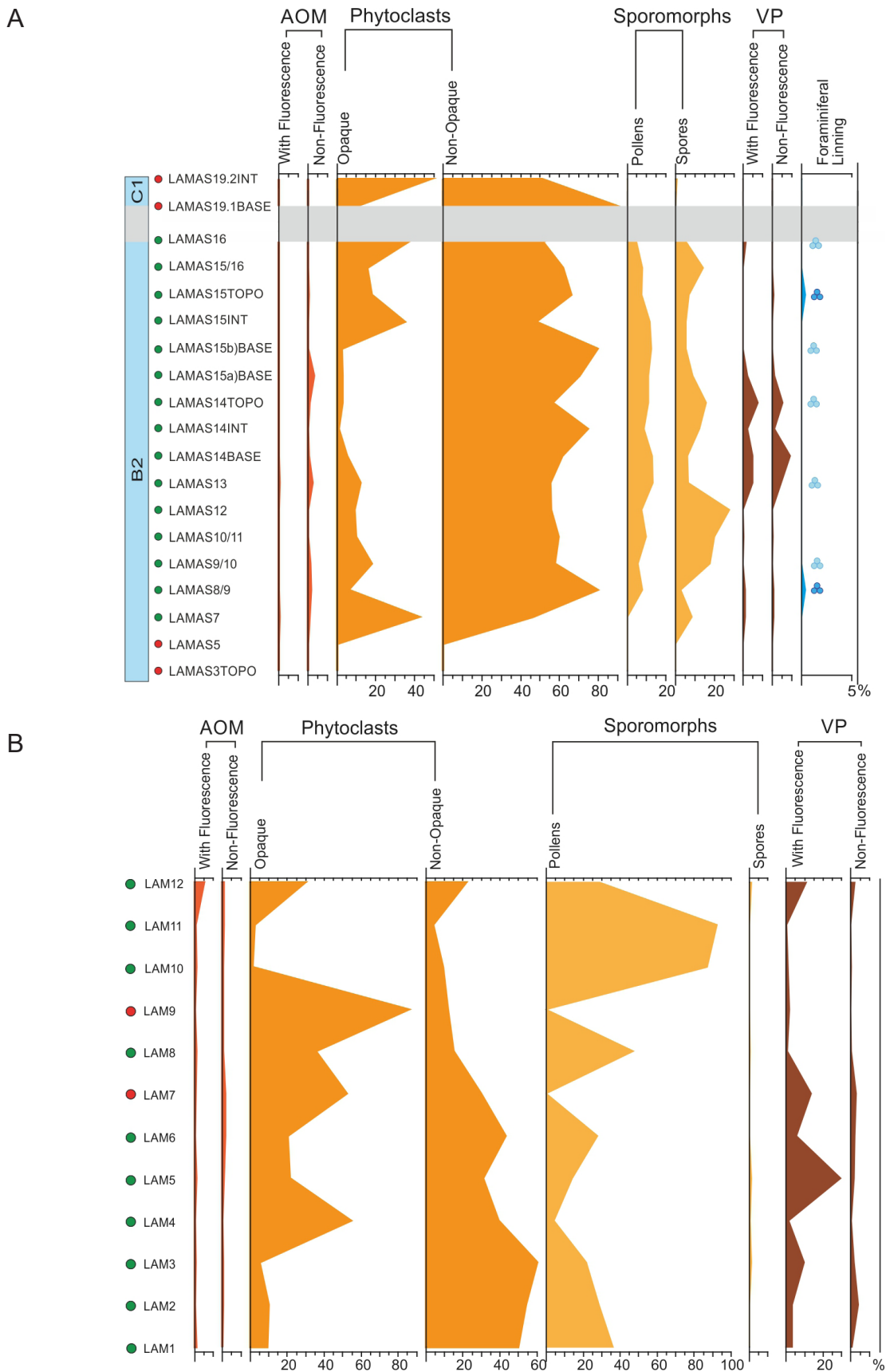


**Figure 8.** Palynofacies analysis along the sections. **A.** Range chart of Lamas I outcrop. The blue symbol marks the samples that contain microforaminifera linings; **B.** Range chart of Lamas II. AOM – Amorphous organic matter. VP – Vegetal particles. Green dots indicate productive samples for palynological studies, and red dots indicate barren samples for palynological studies. The symbols of the foraminifera linings in dark blue represent the samples in which these particles were part of the counts. The symbols in light blue represent the samples that contain foraminifera; however, they did not appear in the analysis of palynofacies. Not to scale

occurrence of *P. longdonensis* in the Hettangian (upper part of the *K. reissingeri* Zone) was documented in Spain, where this taxon occurs with *Pinuspollenites minimus* and *Cerebropollenites thiergartii* (Barrón et al., 2002, 2006). Other locations in southern Europe where *P. longdonensis* was found in the Hettangian age include northern Germany (Schulz and Heunisch, 2005) and the Vicentinian Alps in Italy (Clement-Westerhof et al., 1974). The presence of *Paracirculina* sp., a typical Upper Triassic species, and the fact that there is an acme of lycopodiophyte spores (e.g. *Kraeuselisporites reissingeri*) in the Lamas I section when compared to Lamas II section place the former in a lower position, the base of the Hettangian, agreeing with the stratigraphic interpretation (Cirilli, 2010).

The presence of foraminifera linings in the Lamas I section is noteworthy, even though it does not contribute information to the age discussion.

Several Hettangian key taxa are missing in the studied sections. *Cerebropollenites thiergartii*, the critical marker taxon of the Hettangian age, is not present in the studied sections in the Lusitanian Basin (Vilas-Boas et al., 2021). The presence of *C. thiergartii* marks the base of the Jurassic but is very rare and hard to recognize (Lindström et al., 2017b). However, it may not be a reliable taxon because its FO seems not to be synchronous, varying between localities (Heunisch et al., 2010; Cirilli et al., 2015, 2018; Lindström et al., 2016, 2017b; Panfili et al., 2019). The regression-transgression ‘couplet’ may influence the FO of *C. thiergartii* (Lindström et al., 2017b).

Several authors discussed this issue; for example, Van de Schootbrugge et al. (2009) and Schobben et al. (2019) reported from the Central European Basin (Germany, Sweden, and Bonenburg) a floral transition characterised by a gradual decline in Rhaetian pollen grains, including *Rhaetipollis germanicus*, until they disappeared, being replaced in the early Hettangian by assemblages containing abundant *Classopollis* spp., *Perinopollenites elatoides*, *Pinuspollenites minimus* and bisacates (e.g. *Alisporites* spp.) accompanied by the *Kraeuselisporites reissingeri* acme.

In the GSSP Kuhjoch section for the TJB, the *Trachysporites-Pinuspollenites* Zone (TPi Zone) assigned to the Hettangian age is distinguished by a marked increase in the abundance

of *P. minimus*, which was previously present in low abundance in the underlying TH zone, as well as by the abundance of *Ricciisporites tuberculatus* and *K. reissingeri* together with *Classopollis* spp. and *Trachysporites* spp. (Hillebrandt et al., 2013).

## DEPOSITIONAL SETTING

There are few sedimentological studies carried out in the Silves Group. Thus, the depositional interpretations are based on the classic works of sedimentology and allostratigraphy by Palain (1976, 1979) based on the description of megasequences, complemented by Soares et al. (2012). The two studied sections form a composite succession with a thickness of ~40 m [which include the units B2, C1 and C2 in Palain (1976, 1979)], enabling us to envisage the probable depositional environments during the early Jurassic times based on studies of palynology and palynofacies compared with lithofacies.

## PALYNOFACIES DATA

### Unit B2

The phytoclast group dominates this unit, and the percentage between opaque and non-opaque phytoclasts are related, as one increases when the other decreases. The moderate percentage of spores and pollen grains does not vary much throughout the unit, with spores dominating over pollen grains. The constant presence of foraminifera linings indicates marine water influence. The overall high proportion of continental organic debris (e.g. phytoclasts, vegetable particles, sporomorphs) on marine elements points to a coastal environment. It also fits with lithofacies, mainly consisting of coarse to medium-grained plane-bedded sandstones alternating with carbonate (mostly dolostone).

The low percentage of AOM throughout the entire unit indicates well-oxygenated conditions, as expected along a coastal environment, but the presence of three intervals of dark mudstone-siltstones characterised by a relatively higher content of non-fluorescent AOM, which can be related to the presence of coastal swamps and ponds. In such conditions, the stagnant waters could preserve the AOM, trapped within fine-grained sediments, by strong oxidation processes.

### Unit C1

The palynofacies elements of this lithofacies are strongly oxidised and characterised by the only presence of phytoclasts. This siliciclastic unit, composed chiefly of mature arkosic sandstones, shows sedimentary structures, such as erosive channel surfaces, cross-bedded sandstones, hummocky and herringbone structures. The depositional setting is strongly influenced by river flow, as documented by the frequency of channelized deposits. On the other side, the proximity to the marine environment is testified by the presence of the herringbone structures indicating bidirectional flows such as tidal currents. For unit B2 the depositional setting records a regression of the coastal line. The high energy, high oxygenated conditions and the temporarily prolonged subaerial exposures could be responsible for the organic matter's strong oxidation.

### Unit C2

In most part of the unit C2, the phytoclast group is the most representative group as in the other units the presence of pollen grains is very significant which could indicate a depositional environment close to the parent flora. Compared with lithofacies, the palynofacies features confirm the previous attribution to a lagoonal-tidal flat setting with mixed siliciclastic-carbonate and evaporite deposits (Soares et al., 2012). The warm-arid conditions are supported by the presence, in the recorded palynological assemblage, of abundant *Classopollis meyerianus* and *Classopollis torosus* together with common *Deltoideospora* sp., that have a preference for drier and warmer conditions, with xerophytic microflora as *Alisporites* sp., *Pinuspollenites minimus* and *Porcellispora longdonensis*.

Although the marine influence is expected on a tidal flat, foraminifera linings are absent. It could be explained by the presence of hypersaline waters that prevent the settling of foraminifera. The decrease of phytoclasts and the increase of sporomorphs (mostly pollen grains) and vegetal particles in the uppermost portion of unit C2 suggest more proximity of the depositional environment to the parent flora.

Compared with lithofacies, the palynofacies variations across the composite section point to a depositional environment ranging from coastal to tidal flat in response to short-lived, marine transgression-regression

events. Furthermore, the palynological assemblages and lithofacies indicate a shift towards a warm-arid climate in the upper Hettangian (unit C2).

The facies transition between units B1 and B2 has been interpreted as the first mainly flooding event in the LB based on the mollusc fauna of *Promathildia* and *Isocyprina* in unit B2 (e.g. Soares et al., 1993; Azerêdo et al., 2003). The evidence of the first marine transgressive episode in unit B2 is now further supported by abundant foraminifera linings recorded within the grey to blackish lutites in the lower part of the sequence.

The short-lived marine transgression phase recorded in B2 could be tentatively related to tectonics rather than only eustatic sea-level fluctuations (Hallam, 1981; Haq et al., 1988; Rasmussen et al., 1998).

Hence, we suggest that the tectonism associated with the first rifting phases of the Lusitanian Basin created areas of low topography with embayments that sea waters could more easily inundate. These embayments may have been similar to estuaries where the lower energy conditions in the central basin promote the deposition of fine-grained sediments. Estuarine depositional systems are associated with brackish waters, which explains the presence of foraminifera linings as also recorded in modern estuarine settings in the Iberian Peninsula (Leorri and Cearreta, 2009; Schönfeld and Mendes, 2022). A high percentage of continental-derived OM (e.g. phytoclasts, pollen grains and spores, vegetal particles) were transported and deposited by rivers into an estuarine-type sedimentary environment.

The lower Jurassic transgressive phase followed that recognised in Europe and Canadian Arctic (Embry and Suneby, 1994; Hallam, 1997; Aurell et al., 2003; Gomes and Goy, 2005). According to Hallam et al. (2004), a similar pattern of successive sea-level fall and rise can also be observed in Europe's north and south Triassic–Jurassic sequences; however, like the LB, the upper Rhaetian is missing in southern Sweden and NW Poland, due to the presence of an unconformity at the base of the Jurassic strata (Hallam et al., 2004).

Unit C1 could be interpreted as deposited during a successive rapid sea-level fall, followed by a new episode of transgression under more arid climate conditions with the deposition of unit C2. According to Soares et al.



(2012), this unit records sedimentary processes in an evaporitic tidal flat environment that pass upwards to lacustrine facies, delimited by shoals or sandy bars of laminated “dolomitic” sediments (Soares et al., 2012). The equivalent lateral saline units from the Dagorda Formation can explain the early dolomitization processes affecting unit C2 (Soares et al., 2012). It is worth noting in this unit the sporadic occurrence of *Isocyprina*, which testifies to an environment, locally, not so different from that of unit B2 (Azerêdo et al., 2003).

## CONCLUSIONS

The palynological data allow us to conclude that the two studied sections belong to the Pereiros Formation and are of early Hettangian age, Early Jurassic. This age is confirmed by the presence of the spores *Calamospora tener*, *Ischyosporites variegatus*, *Kraeuselisporites reissingeri* and *Porcellispora longdonensis* and the pollen grains *Alisporites* sp., *Perinopollenites elatoides* and *Pinuspollenites minimus* in both sections.

After analysing the data obtained from the palynology and palynofacies studies, we can conclude that:

- In **unit B2**, *Carnisporites spiniger*, *Kraeuselisporites reissingeri* and *Ischyosporites variegatus* spores and pollen grains *Pinuspollenites minimus*, *Perinopollenites elatoides*, and the dominance of *Classopollis meyerianus* allow dating this unit to the base of the Hettangian. The presence of foraminiferal linings documents, in this unit, the first event of marine flooding occurred in the Lusitanian Basin. The data allow the interpretation of this unit as an estuarine-type environment, suggesting a short-lived marine transgression event;

- **Unit C1** is interpreted as a river-dominated coastal environment with episodes of tidal current influence and records a short regression episode;

- **Unit C2**, the presence of *Kraeuselisporites reissingeri* and *Ischyosporites variegatus* and pollen grains *Perinopollenites elatoides*, *Pinuspollenites minimus* and the dominance of *Classopollis meyerianus* indicate a Hettangian age for this unit. Palynofacies, dominated by pollen grains and phytoclasts, and lithofacies point to an evaporitic tidal flat under warm-arid climate conditions.

We can conclude that marine-marginal depositional settings dominated the Lusitanian Basin during the Hettangian and were interrupted by river-dominated episodes related to the short-lived regressive phase.

The microflora assemblages from the Lusitanian Basin recorded along the Early Jurassic times might shed new light on future palaeogeographical and paleoclimatic reconstructions of this sector of the Tethys realm. Nevertheless, more studies are needed to enhance this further information.

## ACKNOWLEDGEMENTS

MVB is a PhD student at the University of Algarve, with an SFRH/BD/144125/2019 scholarship awarded by the Portuguese Foundation for Science and Technology. The authors would like to acknowledge the funding provided by FCT to the projects LA/P/0069/2020, awarded to the Associate Laboratory ARNET and UIDP/00350/2020, awarded to CIMA of the University of the Algarve. SC acknowledges MIUR project PRIN 2017RX9XXXY and the Research Funds 2021 (University of Perugia), Action Line: Climate, Energy and Mobility – WP5.2, Climate changes: scientific models, technology and social impacts.

## REFERENCES

- Adloff, M.C., Doubinger, J., Palain, C., 1974. Contribution à la palynologie du Trias et du Lias inférieur du Portugal. «Grés de Silves» du Nord du Tage. Comunicações Serviços Geológicos Portugal LVIII, 91–144.
- Arche, A., López-Gómez, J., 2014. The Carnian Pluvial Event in Western Europe: new data from Iberia and Correlation with the Western Neotethys and Eastern North America–NW Africa regions. *Earth-Science Reviews* 128, 196–231. <https://doi.org/10.1016/j.earscirev.2013.10.012>
- Aurell, M., Robles, S., Bádenas, B., Rosales, I., Quezada, S., Meléndez, G., García-Ramos, J.C., 2003. Transgressive–regressive cycles and Jurassic palaeogeography of northeast Iberia. *Sedimentary Geology* 162(3–4), 239–271. [https://doi.org/10.1016/S0037-0738\(03\)00154-4](https://doi.org/10.1016/S0037-0738(03)00154-4)
- Azerêdo, A.C., Duarte, L.V., Henriques, M.H., Manuppella, G., 2003. Da dinâmica continental no Triásico aos mares do Jurássico Inferior e Médio. *Cadernos de Geologia de Portugal*, Instituto Geológico Mineiro, Portugal, p. 43.
- Barbacka, M., Pacyna, G., Kocsis, Á.T., Jarzynka, A., Ziaja, J., Bodor, E., 2017. Changes in terrestrial floras at the Triassic–Jurassic Boundary in Europe. *Palaeogeography, Palaeoclimatology, Palaeoecology* 480, 80–93. <https://doi.org/10.1016/j.palaeo.2017.05.024>

- Barrón, E., Gómez, J.J., Goy, A., 2002. Los materiales del tránsito Triásico–Jurásico en la región de Villaviciosa (Asturias, España). *Caracterización palinológica*. *Geogaceta* 31, 197–200.
- Barrón, E., Gómez, J.J., Goy, A., Pieren, A.P., 2006. The Triassic–Jurassic boundary in Asturias (northern Spain): palynological characterisation and facies. *Review of Palaeobotany and Palynology* 138(3–4), 187–208. <https://doi.org/10.1016/j.revpalbo.2006.01.002>
- Capriolo, M., Marzoli, A., Aradi, L.E., Callegaro, S., Dal Corso, J., Newton, R.J., Mills, B.J.W., Wignall, P.B., Bartoli, O., Baker, D.R., Youbi, N., Remusat, L., Spiess, R., Szabó, C., 2020. Deep CO<sub>2</sub> in the end-Triassic Central Atlantic Magmatic Province. *Nature Communications* 11(1), 1–11. <https://doi.org/10.1038/s41467-020-15325-6>
- Carvalho, G.S., 1950. Considerações sobre a estratigrafia das formações mais antigas da orla mesozoica ocidental de Portugal. *Revista Faculdade Ciências Universidade Coimbra* 19, 39–48.
- Cirilli, S., 2010. Upper Triassic–lowermost Jurassic palynology and palynostratigraphy: a review. *Geological Society, London, Special Publications* 334(1), 285–314.
- Cirilli, S., Marzoli, A., Tanner, L., Bertrand, H., Buratti, N., Jourdan, F., Bellieni, G., Kontak, D., Renne, P.R., 2009. Latest Triassic onset of the Central Atlantic magmatic province (CAMP) volcanism in the Fundy basin (Nova Scotia): new stratigraphic constraints. *Earth and Planetary Science Letters* 286(3–4), 514–525. <https://doi.org/10.1016/j.epsl.2009.07.021>
- Cirilli, S., Buratti, N., Gugliotti, L., Frixia, A., 2015. Palynostratigraphy and palynofacies of the Upper Triassic Streppenosa Formation (SE Sicily, Italy) and inference on the main controlling factors in the organic rich shale deposition. *Review of Palaeobotany and Palynology* 218, 67–79. <https://doi.org/10.1016/j.revpalbo.2014.10.009>
- Cirilli, S., Panfili, G., Buratti, N., Frixia, A., 2018. Paleoenvironmental reconstruction by means of palynofacies and lithofacies analyses: an example from the Upper Triassic subsurface succession of the Hyblean Plateau Petroleum System (SE Sicily, Italy). *Review of Palaeobotany and Palynology* 253, 70–87. <https://doi.org/10.1016/j.revpalbo.2018.04.003>
- Clement-Westerhof, J.A., Van Der Eem, J.G.L.A., Van Erve, A.W., Klasen, J.J., Schuurman, W.M.L., Visscher, H., 1974. Aspects of Permian, Triassic and Early Jurassic palynology of western Europe – a research project. *Geologie en Mijnbouw* 53(6), 329–341.
- Curtis, R., Evans, G., Kinsmann, D.J.J., Shearman D.J., 1963. Association of dolomite and anhydrite in recent sediments of the Persian Gulf. *Nature*, 196, 679–680. <https://doi.org/10.1038/197679a0>
- Davies, J.H.F.L., Marzoli, A., Bertrand, H., Youbi, N., Ernesto, M., Schaltegger, U., 2017. End-Triassic mass extinction started by intrusive CAMP activity. *Nature Communications* 8, 1–8. <https://doi.org/10.1038/ncomms15596>
- Deenen, M.H., Ruhl, M., Bonis, N.R., Krijgsman, W., Kürschner, W.M., Reitsma, M., Van Bergen, M.J., 2010. A new chronology for the end-Triassic mass extinction. *Earth and Planetary Science Letters* 291(1–4), 113–125. <https://doi.org/10.1016/j.epsl.2010.01.003>
- Díez, J.B., 2000. *Geología y Paleobotánica de la facies Buntsandstein en la Rama Aragonesa de la Cordillera Ibérica*. Implicaciones bioestratigráficas en el Peritethys occidental. Unpublished PhD Thesis, Univ. de Zaragoza/Univ. Pierre et Marie Curie-París-6.
- Dimuccio, L.A., Duarte, L.V., Cunha, L., 2014. Facies and stratigraphic controls of the palaeokarst affecting the Lower Jurassic Coimbra Group, Western Central Portugal. In: Rocha, R.B., Pais, J., Kullberg, J.C., Finney, S. (Eds), *Strati 2013*. First International Congress on stratigraphy. At the cutting edge of Stratigraphy. *Springer Geology XLV*, pp. 787–791.
- Dimuccio, L.A., Duarte, L.V., Cunha, L., 2016. Definição litostratigráfica da sucessão calcodolomítica do Jurássico Inferior da região de Coimbra-Penela (Bacia Lusitânica, Portugal). *Comunicações Geológicas* 103(1), 77–96.
- Doubinger, J., Adloff, M., Palain, C., 1970. Nouvelles précisions stratigraphiques sur la série de base du Mésozoïque portugais. *Comptes Rendus Académie des Sciences Paris* 270, 1770–1772.
- Duarte, L.V., Silva, R.L., Azerêdo, A.C., Comas-Rengifo, M.J., Mendonça Filho, J.G., 2022. Shallow-water carbonates of the Coimbra Formation, Lusitanian Basin (Portugal): contributions to the integrated stratigraphic analysis of the Sinemurian sedimentary successions in the western Iberian Margin. *Comptes Rendus Géoscience* 354(S3), 1–18. <https://doi.org/10.5802/crgeos.144>
- Embry, A.F., Suneby, L.B., 1994. The Triassic–Jurassic boundary in the Sverdrup Basin, Arctic Canada. *Canadian Society of Petroleum Geologists Memoir* 17, 857–868.
- Gradstein, F.M., Ogg, J.G., 2020. The chronostratigraphic scale. *Geologic Time Scale 2020*. Elsevier, pp. 21–32.
- Grimm, E.C., 1991. *TILIA and TILIAGRAPH*. PC Spreadsheet and Graphics Software for Pollen Data. INQUA Working Group on Data Handling Methods.
- Gómez, J.J., Goy, A., 2005. Late Triassic and Early Jurassic palaeogeographic evolution and depositional cycles of the Western Tethys Iberian platform system (Eastern Spain). *Palaeogeography, Palaeoclimatology, Palaeoecology* 222(1–2), 77–94.
- Gómez, J.J., Aguado, R., Azerêdo, A.C., Cortés, J.E., Duarte, L.V., O'Dogherty, L., Rocha, R.B., Sandoval, J., 2019. The Late Triassic–Middle Jurassic Passive Margin Stage. *The Geology of Iberia: A Geodynamic Approach: Volume 3: The Alpine Cycle*, 113–167.

- Guex, J., Bartolini, A., Atudorei, V., Taylor, D., 2004. High-resolution ammonite and carbon isotope stratigraphy across the Triassic–Jurassic boundary at New York Canyon (Nevada). *Earth and Planetary Science Letters* 225, 29–41. <http://dx.doi.org/10.1016/j.epsl.2004.06.006>
- Hallam, A., 1981. A revised sea-level curve for the early Jurassic. *Journal of the Geological Society* 138(6), 735–743. <https://doi.org/10.1144/gsjgs.138.6.0735>
- Hallam, A., 1997. Estimates of the amount and rate of sea-level change across the Rhaetian–Hettangian and Pliensbachian–Toarcian boundaries (latest Triassic to early Jurassic). *Journal of the Geological Society* 154(5), 773–779. <https://doi.org/10.1144/gsjgs.154.5.0773>
- Hallam, T., Wignall, P., Hesselbo, S.P., Robinson, S.A., Surlyk, F., 2004. Discussion on sea-level change and facies development across potential Triassic–Jurassic boundary horizons, SW Britain. *Journal of the Geological Society* 161(6), 1053–1056. <https://doi.org/10.1144/0016-764904-069>
- Haq, B.U., Hardenbol, J., Vail, P.R., 1988. Mesozoic and Cenozoic chronostratigraphy and cycles of sea-level change. *Society of Economic Paleontologists and Mineralogists Special Publication* 42, 71–108.
- Hesselbo, S.P., Robinson, S.A., Surlyk, F., Piasecki, S., 2002. Terrestrial and marine extinction at the Triassic–Jurassic boundary synchronized with major carbon-cycle perturbation: a link to initiation of massive volcanism? *Geology* 30(3), 251–254. [https://doi.org/10.1130/0091-7613\(2002\)030%3C0251:TAMEAT%3E2.0.CO;2](https://doi.org/10.1130/0091-7613(2002)030%3C0251:TAMEAT%3E2.0.CO;2)
- Heunisch, C., Luppold, F.W., Reinhardt, L., Röhling, H.-G., 2010. Palynofazies, Bio-und Lithostratigraphie im Grenzbereich Trias/Jura in der Bohrung Mariental 1 (Lappwaldmulde, Ostniedersachsen). *Zeitschrift der Deutschen Gesellschaft für Geowissenschaften* 161, 51–98.
- Hillebrandt, A.V., Krystyn, L., Kürschner, W.M., Bonis, N.R., Ruhl, M., Richoz, S., Schobben, M.A.N., Urlichs, M., Bown, P.R., Kment, K., McRoberts, C.A., Simms, M., Tomášovych, A., 2013. The Global Stratotype Sections and Point (GSSP) for the base of the Jurassic Systemat Kuhjoch (Karwendel Mountains, Northern Calcareous Alps, Tyrol, Austria). *Episodes* 36, 162–198. <https://doi.org/10.18814/epiugs/2013/v36i3/001>
- Hiscott, R.N., Wilson, R.C., Gradstein, F.M., Pujalte, V., Garcia-Mondéjar, J., Boudreau, R.R., Wishart, H.A., 1990. Comparative stratigraphy and subsidence history of Mesozoic rift basins of North Atlantic. *AAPG Bulletin* 74(1), 60–76. <https://doi.org/10.1306/0C9B2213-1710-11D7-8645000102C1865D>
- Kullberg, J.C., Rocha, R.B., Soares, A.F., Rey, J., Terreira, P., Azerêdo, A.C., Callapez, P., Duarte, L.V., Kullberg, M.C., Martins, L., Miranda, R., Alves, C., Mata, J., Madeira, J., Mateus, O., Moreira, M., Nogueira, C.R., 2013. A Bacia Lusitaniana: estratigrafia paleogeografia e tectónica. In: Dias, R., Araújo, A., Terreira, P., Kullberg, J.C. (Eds), *Geologia de Portugal. Vol. II. Livraria Escolar Editora*, pp. 195–347.
- Leorri, E., Cearreta, A., 2009. Recent sea-level changes in the southern Bay of Biscay: transfer function reconstructions from salt-marshes compared with instrumental data. *Scientia Marina* 73(2), 287–296. <https://doi.org/10.3989/scimar.2009.73n2287>
- Lindström, S., 2016. Palynofloral patterns of terrestrial ecosystem change during the end-Triassic event – a review. *Geological Magazine* 153(2), 223–251. <https://doi.org/10.1017/S0016756815000552>
- Lindström, S., Erlström, M., Piasecki, S., Nielsen, L.H., Mathiesen, A., 2017a. Palynology and terrestrial ecosystem change of the Middle Triassic to lowermost Jurassic succession of the eastern Danish Basin. *Review of Palaeobotany and Palynology* 244, 65–95. <https://doi.org/10.1016/j.revpalbo.2017.04.007>
- Lindström, S., Van De Schootbrugge, B., Hansen, K.H., Pedersen, G.K., Alsen, P., Thibault, N., Dybkjær, K., Bjerrum, C.J., Nielsen, L.H., 2017b. A new correlation of Triassic–Jurassic boundary successions in NW Europe, Nevada and Peru, and the Central Atlantic Magmatic Province: a time-line for the end-Triassic mass extinction. *Palaeogeography, Palaeoclimatology, Palaeoecology* 478, 80–102. <https://doi.org/10.1016/j.palaeo.2016.12.025>
- Lindström, S., Sanei, H., Van De Schootbrugge, B., Pedersen, G.K., Leshner, C.E., Tegner, C., Heunisch, C., Dybkjær, K., Outridge, P.M., 2019. Volcanic mercury and mutagenesis in land plants during the end-Triassic mass extinction. *Science Advances* 5 (10), eaaw4018. <https://doi.org/10.1126/sciadv.aaw4018>
- Lindström, S., Callegaro, S., Davies, J., Tegner, C., van de Schootbrugge, B., Pedersen, G.K., Youbi, N., Sanei, H., Marzoli, A., 2021. Tracing volcanic emissions from the Central Atlantic Magmatic Province in the sedimentary record. *Earth-Science Reviews* 212, 103444. <https://doi.org/10.1016/j.earscirev.2020.103444>
- Martins, L.T., Madeira, J., Youbi, N., Munhá, J., Mata, J., Kerrich, R., 2008. Rift-related magmatism of the Central Atlantic magmatic province in Algarve, southern Portugal. *Lithos* 101, 102–124. <https://doi.org/10.1016/j.lithos.2007.07.010>
- Marzoli, A., Bertrand, H., Knight, K.B., Cirilli, S., Buratti, N., Vérati, C., Nomade, S., Renne, P.R., Youbi, N., Martini, R., Allenbach, K., Neuwerth, R., Rapaille, C., Zaninetti, L., Bellieni, G., 2004. Synchrony of the Central Atlantic magmatic province and the Triassic–Jurassic boundary climatic and biotic crisis. *Geology* 32, 973–976.
- Mazzullo, S.J., 2000. Organogenic dolomitization in peritidal to deep-sea sediments. *Journal of Sedimentary Research* 70(1), 10–23. <https://doi.org/10.1306/2DC408F9-0E47-11D7-8643000102C1865D>
- Nomade, S., Knight, K.B., Beutel, E., Renne, P.R., Verati, C., Féraud, G., Marzoli, A., Youbi, N., Bertrand, H., 2007. Chronology of the Central Atlantic



- Magmatic Province: implications for the Central Atlantic rifting processes and the Triassic–Jurassic biotic crisis. *Palaeogeography, Palaeoclimatology, Palaeoecology* 244(1–4), 326–344. <https://doi.org/10.1016/j.palaeo.2006.06.034>
- Palain, C., 1976. Une série détritique terrigène les «Grès de Silves»: Trias et Lias inférieur du Portugal. *Memórias Serviços Geológicos Portugal* 25, 377.
- Palain, C., 1979. Connaissances stratigraphiques sur la base du Mésozoïque portugais. *Ciências da Terra* 5, 11–28.
- Panfili, G., Cirilli, S., Dal Corso, J., Bertrand, H., Medina, F., Youbi, N., Marzoli, A., 2019. New biostratigraphic constraints show rapid emplacement of the Central Atlantic Magmatic Province (CAMP) during the end-Triassic mass extinction interval. *Global and Planetary Change* 172, 60–68. <https://doi.org/10.1016/j.gloplacha.2018.09.009>
- Paterson, N.W., Mangerud, G., 2020. A revised palynozonation for the Middle–Upper Triassic (Anisian–Rhaetian) series of the Norwegian Arctic. *Geological Magazine* 157(10), 1568–1592. <https://doi.org/10.1017/S0016756819000906>
- Rasmussen, E.S., Lomholt, S., Andersen, C., Vejbak, O.V., 1998. Aspects of the structural evolution of the Lusitanian Basin in Portugal and the shelf and slope area offshore Portugal. *Tectonophysics* 300, 199–255. [https://doi.org/10.1016/S0040-1951\(98\)00241-8](https://doi.org/10.1016/S0040-1951(98)00241-8)
- Raup, D.M., Sepkoski, J.J., 1982. Mass extinction in the marine fossil record. *Science* 215, 1501–1503. <https://doi.org/10.1126/science.215.4539.1501>
- Riding, J.B., Warny, S., 2008. Palynological techniques. Second edition. American Association of Stratigraphic Palynologists Foundation, Dallas, Texas, p. 137.
- Schaltegger, U., Guex, J., Bartolini, A., Schoene, B., Ovtcharova, M., 2008. Precise U–Pb age constraints for end-Triassic mass extinction, its correlation to volcanism and Hettangian post-extinction recovery. *Earth and Planetary Science Letters* 267, 266–275. <https://doi.org/10.1016/j.epsl.2007.11.031>
- Schneebeli-Hermann, E., Looser, N., Hochuli, P.A., Furrer, H., Reisdorf, A.G., Wetzel, A., Bernasconi, S.M., 2018. Palynology of Triassic–Jurassic boundary sections in northern Switzerland. *Swiss Journal of Geosciences* 111(1–2), 99–115. <https://doi.org/10.1007/s00015-017-0286-z>
- Schobben, M., Van De Schootbrugge, B., Wignall, P.B., 2019. Interpreting the carbon isotope record of mass extinctions. *Elements* 15(5), 331–337. <https://doi.org/10.2138/gselements.15.5.331>
- Schönfeld, J., Mendes, I., 2022. Benthic foraminifera and pore water carbonate chemistry on a tidal flat and salt marsh at Ria Formosa, Algarve, Portugal. *Estuarine, Coastal and Shelf Science* 276, 108003. <https://doi.org/10.1016/j.ecss.2022.108003>
- Schulz, E.K., Heunisch, C., 2005. Palynostratigraphische Gliederungsmöglichkeiten des deutschen Keupers. In: Beutler, G., et al. (Eds), *Stratigraphie von Deutschland IV*. Courier Forschungsinstitut Senckenberg 253, 43–49.
- Sêco, S.L.R., Duarte, L.V., Pereira, A.J.S.C., 2015. Utilização da espectrometria gama na caracterização das unidades da base do Jurássico Inferior do sector norte da Bacia Lusitânica (Portugal): dados preliminares. *Comunicações Geológicas* 102 (Especial I), 41–44.
- Sepkoski, J.J., 1996. Patterns of Phanerozoic extinction: A perspective from global data bases. In: Waliser, O.H. (Ed.), *Global Events and Event Stratigraphy*. Springer-Verlag, Berlin, pp. 35–51.
- Shinn, E.A., 1983. Tidal flat environment. In: Scholle, P.A., Bebout, D.G., Moore, C.H. (Eds), *Carbonate depositional environments*. AAPG Memories 33, 173–210.
- Soares, A.F., Rocha, R.B., Elmi, S., Henriques, M.H., Mouterde, R., Almeras, Y., Ruget, C., Marques, J.F., Duarte, L.V., Carapito, M.C., Kullberg, J.C., 1993. Le sous-bassin nord-lusitanien (Portugal) du Trias au Jurassique moyen: histoire d’un “rift avorté”. *Comptes Rendus de l’Académie des Sciences, Paris (II)* 317, 1659–1666.
- Soares, A.F., Marques, J.F., Sequeira, A., 2007. Carta Geológica de Portugal Folha 19-D (Coimbra-Lousã) à escala 1:50 000. Notícia Explicativa da Folha 19-D (Coimbra-Lousã). Lisboa, Instituto Nacional de Engenharia Tecnologia e Inovação.
- Soares, A.F., Kullberg, J.C., Marques, J.F., da Rocha, R.B., Callapez, P.M., 2012. Tectono-sedimentary model for the evolution of the Silves Group (Triassic, Lusitanian basin, Portugal). *Bulletin de la Société Géologique de France* 183(3), 203–216. <https://doi.org/10.2113/gssgfbull.183.3.203>
- Tanner, L.H., Lucas, S.G., Chapman, M.G., 2004. Assessing the record and causes of Late Triassic extinctions. *Earth-Science Review* 65, 103–139. [https://doi.org/10.1016/S0012-8252\(03\)00082-5](https://doi.org/10.1016/S0012-8252(03)00082-5)
- Tanner, L.H., Smith, D.L., Allan, A., 2007. Stomatal response of swordfern to volcanogenic CO<sub>2</sub> and SO<sub>2</sub> from Kilauea volcano, Hawaii. *Geophysical Research Letters* 34, L15807. <https://doi.org/10.1029/2007GL030320>
- Teixeira, C., 1942. Notas sobre a geologia do Triássico português. *Boletim Sociedade Geológica Portugal* Vol. 1, Fasc. III, 161–175.
- Tyson, R.V., 1993. Chapter 5: palynofacies analysis. In: Jenkins, D.G. (Ed.), *Applied Micropaleontology*. Kluwer Academic Publishers, The Netherlands, Amsterdam, pp. 153–191.
- Tyson, R.V., 1995. *Sedimentary Organic Matter. Organic Facies and Palynofacies*. Chapman and Hall, Londres, p. 615.
- Van De Schootbrugge, B., Payne, J.L., Tomasovych, A., Pross, J., Fiebig, J., Benbrahim, M., Föllmi, K.B., Quan, T.M., 2008. Carbon cycle perturbation and stabilization in the wake of the Triassic–Jurassic boundary mass-extinction event. *Geochemistry, Geophysics, Geosystems* 9(4), 1–16. <https://doi.org/10.1029/2007GC001914>

- Van De Schootbrugge, B., Quan, T.M., Lindström, S., Puttmann, W., Heunisch, C., Pross, J., Fiebig, J., Petschick, R., Rohling, H., Richoz, S., Rosenthal, Y., Falkowski, P.G., 2009. Floral changes across the Triassic–Jurassic boundary linked to flood basalt volcanism. *Nature Geoscience* 2(8), 589–594. <https://doi.org/10.1038/ngeo577>
- Verati, C., Rapaille, C., Féraud, G., Marzoli, A., Bertrand, H., Youbi, N., 2007.  $^{40}\text{Ar}/^{39}\text{Ar}$  ages and duration of the Central Atlantic Magmatic Province volcanism in Morocco and Portugal and its relation to the Triassic–Jurassic boundary. *Palaeogeography, Palaeoclimatology, Palaeoecology* 244(1–4), 308–325. <https://doi.org/10.1016/j.palaeo.2006.06.033>
- Vigran, J.O., Mangerud, G., Mørk, A., Worsley, D., Hochuli, P.A., 2014. Palynology and geology of the Triassic succession of Svalbard and the Barents Sea. *Geological Survey of Norway Special Publication* 14, 1–270.
- Vilas-Boas, M., Pereira, Z., Cirilli, S., Duarte, L.V., Fernandes, P., 2021. New data on the palynology of the Triassic–Jurassic boundary of the Silves Group, Lusitanian Basin, Portugal. *Review of Palaeobotany and Palynology* 290, 104426. <https://doi.org/10.1016/j.revpalbo.2021.104426>
- Wilson, R.C.L., 1975. Atlantic opening and Mesozoic continental margin basins of Iberia. *Earth and Planetary Science Letters* 25(1), 33–43. [https://doi.org/10.1016/0012-821X\(75\)90207-1](https://doi.org/10.1016/0012-821X(75)90207-1)
- Wilson, M., Giraud, R., 1998. Late Permian to recent magmatic activity on the African–Arabian margin of Tethys. In: MacGregor, D., Moody, R., Clark-Lowes, D. (Eds), *Petroleum Geology of North Africa*. Geological Society, London, Special Publications, vol. 132, pp. 231–263.
- Wood, G.D., Gabriel, A.M., Lawson, J.E., 1996. Palynological techniques processing and microscopy. In: Jansonius, J., McGregor, D.C. (Eds), *Palynology: Principles and applications*. 1. American Association Stratigraphic Palynology Foundation, pp. 29–50.